A THERMODYNAMIC CLASSIFICATION OF PHASE TRANSFORMATION INTERFACE MORPHOLOGIES

A THERMODYNAMIC CLASSIFICATION OF PHASE TRANSFORMATION INTERFACE MORPHOLOGIES

By

DONALD G. FEDAK, B. Sc.

A Thesis

Submitted to the Faculty of Graduate Studies

in Partial Fulfilment of the Requirements

for the Degree

Master of Science

McMaster University

May 1961

MASTER OF SCIENCE (1961) MCMASTER UNIVERSITY
(Metallurgy) Hamilton Ontario

TITLE: A Thermodynamic Classification of Phase Transformation Interface Morphologies

AUTHOR: Donald G. Fedak, B. Sc. (McMaster University)

SUPERVISOR: Dr. J. S. Kirkaldy

NUMBER OF PAGES: v, 44.

SCOPE AND CONTENTS:

This thesis examines the factors controlling morphological development at phase transformation interfaces. A morphological classification for phase transformations in condensed systems based on the principle of local equilibrium is presented. Four distinct classes appear. Three of these, liquid - solid transformations in unary and binary systems and solid - solid Widmanstatten type transformations in binary systems have been extensively considered in the literature and are examined here in terms of the proposed thermodynamic classification. A fourth class, involving solid - solid transformations in ternary systems, is seen to follow naturally from the discussion of the former three. The experimental verification of predictions concerning morphological development in this latter class concludes the presentation.

PREFACE

This thesis describes a Master of Science research program of duration May, 1960 to April, 1961 inclusive. It represents part of an extensive research program designed to investigate the thermodynamic aspects of phase transformations. A great deal of effort has been devoted to the application of multicomponent diffusion theory to (de)carburization, pearlite, and segregation reactions; particularly in ferrous alloys. This fundamental research program is here extended to a general study of the morphological aspects of phase transformation interfaces.

Substantially all industrial metallurgical phase transformations are accompanied by the development of non-planar morphologies with attendant segregation. Previous investigations have demonstrated that the factors controlling the type and degree of morphological development are varied and complex. It is apparent that the structural character of an interface is determined, to a large extent, by the system's phasial constitution in terms of the concentration, temperature, and pressure variables. Therefore, an examination of the relation between these parameters and the structural form of non-planar interfaces was suggested as a potentially valuable field of endeavour.

ACKNOWLEDGEMENTS

The thesis is a summary of theoretical and experimental work performed jointly, the author's chief concern having been the experimental verification of predictions arising from the theory. The director's continued advice and assistance during the course of the work is much appreciated.

Thanks are extended to Dr. K. G. Carroll, Dr. B. H. Heise, and Mr. Todd Solberg of International Nickel Company Research Laboratories, Bayonne, New Jersey, U. S. A. for kindly providing valuable electron probe analyses of diffusion couples.

The assistance of Mr. Horst Neumeyer laboratory technician at McMaster University, is gratefully acknowledged.

Financial assistance was provided by an International Nickel Company of Canada graduate fellowship and an American Iron and Steel Institute research grant.

TABLE OF CONTENTS

INTRODUCTION

Non-planar morphological development is experimentally common at the interface in unidirectionally transforming two-phase systems. Three distinctly different systems appear to develop stable non-planar interfaces.

1 - Pure Metal Solidification

Solidification in pure substances often proceeds by unidirectional conduction of heat through the already transformed solid and its container. A typical relationship between temperature and distance is represented by Figure 1 (a).[1] A minute amount of supercooling of the liquid ahead of the interface, dT_{SC}, is necessary to drive the transformation reaction. Non-planar interfaces are unstable in this case since the nuclei that form on the advancing interface encounter a zone of increased temperature and redissolve. The interface remains essentially planar and advances with the fusion temperature isotherm.

If solidification is accompanied by non-unidirectional heat flow (i. e. heat is lost laterally through the liquid as well as by conduction through the transformed solid) the temperature - distance plot may assume the form of Figure 1 (b). Nuclei that form on an initially planar interface will project into regions of decreased temperature and may continue to grow. According to Rainberg and

(1) References are given at the end of the thesis.

Chalmers [2], as projections increase in length they encounter larger degrees of supercooling and grow more rapidly and at the expense of less advanced neighbouring projections. Non-planar growth will therefore be stable in the presence of a negative temperature gradient ahead of the interface. Protuberances will continue to grow as long as this negative temperature gradient makes possible the establishment of local equilibria between their tips and the adjacent melt.

Figure 2 is a micrograph which illustrates the development of non-planar projections in pure lead and the preferential growth of those which were first to form. Figure 3 shows how an initially stable planar interface may be arranged experimentally to encounter a region of locally supercooled liquid.

2 - Alloy Solidification

During solidification of a binary alloy, interface propagation may be accompanied, as in the previous case, by unidirectional conduction of heat away from the interface through the solid. An actual temperature distribution may be as in Figure 1 (a). The new feature in this case is that there is a redistribution of solute at the interface. A solute gradient is established which can be used to derive from the constitution diagram a local equilibrium temperature profile as in Figure 4 [4]. Interfacial nuclei may become stable when the actual temperature profile is lower than the local equilibrium profile (∇T_{crit} on

Figure 4). Nucleation will be followed by the growth of the projections to some limiting steady-state length.

Non-planar interface development during alloy solidification is controlled directly by locally interacting temperature and concentration gradients. The critical values of these gradients are a direct function of the system's equilibrium constitution diagram.

3 - Widmanstätten Precipitation from Solid Solution

The precipitation of a second phase during the isothermal transformation of a quenched single phase solid solution is similarly controlled by the system's constitutional nature. Local redistribution of solute about an initial nucleus establishes a concentration gradient at the interface. The rate of growth of the interface will be limited by the rate of diffusion of solute to or away from it.

The formation of the nuclei of morphologic units upon the initial precipitate is accompanied by local pressure changes due mainly to the surface tension associated with the small radius of curvature of the new interface. This local pressure change may decrease the equilibrium solute content of the precipitating (and possibly the parent) phase. This is shown schematically by the dotted lines in Figure 5. Figures 6 and 7 illustrate the effect of a local surface tension change on the solute concentration profile in front of an interface. Non-planar growth of Widmanstätten type during isothermal solid - solid transformation is controlled by interacting local concentration and pressure gradients of this type.

Of the above three cases, alloy solidification has been investigated the most extensively. This is due to the fact that the boundary conditions yield to steady state control. The success of the analysis in that case would seem to suggest the value of the pursuit of a general thermodynamic synthesis encompassing all other possible cases. The three cases are variously controlled by

interacting local temperature, pressure and concentration gradients. It appears possible that there are other ways of arranging these gradients to produce stable non-planar morphologies.

Unidirectional growth of one phase into another can take place in a two-phase isothermal diffusion experiment. However, isothermal diffusion in two-phase binary systems cannot produce morphological development. The theoretical justification for this statement is presented later. On the other hand, a thermodynamic argument indicates that a fourth case, isothermal diffusion in two-phase ternary systems, is capable of producing stable non-planar morphological development. Appropriate ternary systems are examined experimentally to verify the occurrence of such stable non-planar transformation interfaces.

HISTORICAL

Pure Metal Solidification

The appearance of cellular and dendritic morphologies during single crystal growth from a supercooled melt has motivated numerous attempts to determine the mechanism operative during solidification.

In 1925, Tammann et al [5] investigated the solidification characteristics of pure organic compounds and observed dendritic and columnar type interfaces. They demonstrated the importance of thermal supercooling as a prerequisite for morphological development.

The works of Stranski [5], Frank [7], and Chalmers et al [8] have respectively called attention to the importance of three possible mechanisms - two-dimensional nucleation, growth by screw dislocation propagation, and growth from reentrant positions. It now seems that these three mechanisms are all operative, either singularly or cooperatively, during transformation.

Weinberg and Chalmers [1,2] have qualitatively explained cellular and dendritic morphological development during pure metal solidification in terms of the thermal gradient at the interface. Experimentally, they observed that stable non-planar morphologies were maintained by a negative temperature gradient in the adjacent melt. The advance of projections was favoured by the presence of

increasingly larger degrees of supercooling. The solidification interface was observed directly after decantation of the melt. Dendrite spacing was observed to be characteristic of and increase directly with the degree of supercooling. They concluded that non-unidirectional heat flow away from the protuberance tip, made possible by a negative temperature gradient, stabilizes non-planar growth.

In retrospect, a complete description of pure substance solidification does not exist. The experimental boundary conditions are unavoidably difficult to examine and control. Latent heat evolution at the interface must be accounted for. At normal levels of purity there may well be substantial redistribution of impurity about the interface. It is quite clear that surface tension will result in the establishment of significant local pressure changes at the tips of projections which will necessarily alter the fusion temperature. In fact, as we shall note later, a non-planar interface is not possible in the absence of surface tension induced local pressure changes. While experimental difficulties have prevented advance in this pure metal configuration, much has been learned through the study of the solidification of alloy single crystals.

Alloy Solidification

The addition of a second element adds a degree of freedom to the case of pure substance solidification. At the same time, it results in a system amenable to experimental control under steady state conditions.

Tiller [4] has expressed mathematically the critical conditions for non-planar interfacial development. He considers the solidification of a binary alloy of initial composition, C_o, in the alloy system typified by Figure 8. Figure 9 represents the variation of solute concentration and the corresponding depression of the equilibrium fusion temperature during steady state growth of an alloy single crystal from the melt.

The concentration of solute in the liquid is proportional to e^{-vx/D_L} and increases from the bulk concentration $C_L(\infty)=C_o$ to the interface concentration $C_L(0)$ in a distance of the order of δ . δ is related to the solute diffusion constant, D_L, and the interface velocity, v, by:

$$\delta = D_L/v \ . \qquad -(1)$$

$C_L(0)=C_o / k_o$, where k_o is the equilibrium partition coefficient as determined from the phase diagram (Figure 8).

The interface solute flux balance gives :

$$\left(\frac{dC_L}{dx}\right)_{x=0} = \frac{-v\,C_L(0)(1-k_o)}{D_L} \qquad -(2)$$

If

$$m = (dT/dC_L) \qquad -(3)$$

then $$\nabla T_E = m\left(\frac{dC_L}{dx}\right)_{x=0} = \left(\frac{dT}{dx}\right)_{x=0} \qquad -(4)$$

is the slope of the equilibrium liquidus temperature distribution and

$$\nabla T/v \leq mC_o(1-k_o)/k_o D_L \qquad -(5)$$

describes the critical conditions necessary for the stabilization of non-planar interfaces during steady state transformations in such systems since it expresses the condition whereby local equilibrium can be sustained along a non-planar interface. Figure 9(c) graphically illustrates a system in which the critical conditions have been satisfied. Experimentally, it has been found that the critical conditions must be greatly exceeded in most cases.

When the critical conditions are exceeded without the formation of interface projections there is established a zone of supersaturation in the melt adjacent to the advancing interface. The extent of the zone varies directly with the interface velocity and inversely with the solute diffusivity. The nucleation of stable non-planar features is encouraged within this metastable region.

In this steady state analysis pressure has been considered to be constant throughout the system. Actually, non-planar development is accompanied by the establishment of local pressure changes due to surface tension. Large pressure changes markedly affect the solubility limits in Figure 8. The importance of these pressure variations during morphological development is stressed

in the next section. They are undoubtedly the cause of the failure to obtain non-planar morphologies without greatly exceeding the critical growth conditions.

Widmanstätten type Precipitation

The formation of needle and plate-like precipitates during the isothermal transformation of quenched alloys has been widely studied.

Dubé [9] devoted considerable effort to a study of the morphological character of proeutectoid precipitates in hypoeutectoid commercial steels. In his examination of the microstructure of quenched polycrystalline γ-phase samples he found that composition, temperature and grain size affect the form of the resultant $\alpha+\gamma$ interface. He classified the precipitate as either massive, grain boundary, or Widmanstätten according to Figure 10.

Later [10,11] this classification was modified to the form outlined in Figure 11.

This classification of precipitate form is apparently characteristic, without modification, of the products of proeutectoid, eutectoid, peritectoid, aging and other diffusion controlled precipitation reactions in a broad range of alloy systems [11]. Examples of Widmanstätten type behavior included in the classification are the precipitation of proeutectoid cementite from hypereutectoid iron-carbon alloys [12] and proeutectoid α-phase precipitation from hypoeutectoid titanium-chromium alloys [11].

Aaronson holds the view that morphological development is not particularly dependent upon either the crystal structures, the compositional differences, the solution types, the types of crystal

bonding, or the mechanisms of nucleation and growth of the matrix and precipitate phases. He chooses rather to discuss the migrational characteristics of phase boundaries in terms of interface structures, nucleation sites, and volume strain energies of transformation. It is suggested that phase boundary propagation is diffusion controlled. The energetic requirements of different nucleation sites seem to determine the ultimate distribution of precipitates as well as their absolute number. Volume strain energies appear to establish local pressure gradients and cause variation of solute concentration, markedly affecting the structural form and stability of precipitate phase boundaries.

Both Zener [13] and Hillert [14] consider the changes in interfacial concentration that result from surface tension in their analyses of the growth of Widmanstätten type precipitates. They assume that the associated local pressure variations do not cause deformation and that local chemical equilibrium is maintained at the interface. The rate of transformation is controlled by diffusion of material subject to interacting pressure and chemical gradients along the interface.

Summary

Although experimental difficulties have discouraged extensive work on the solidification of pure substances it has been demonstrated that non-planar interfacial development is possible

in the presence of a negative temperature gradient at the interface. The problem of alloy solidification has yielded to analysis. It has been demonstrated that morphological development is encouraged by the presence of appropriately arranged interacting temperature and chemical gradients. Work on solid state Widmanstätten type transformation reactions has pointed out the importance of the local pressure gradient and the accompanying interacting chemical gradient in the development of stable non-planar morphologies.

The possible establishment of pressure gradients of sufficient magnitude to affect the configurational nature of pure metal and alloy solidification reactions is suggested by work on Widmanstatten reactions. The final result of such pressure variations is probably a modification in degree of the critical conditions necessary for non-planar development.

THEORY

A Thermodynamic Classification of Morphologies

Locally interacting temperature, pressure, and concentration gradients are known to control non-planar morphological development in three distinctively different systems. The search for a general thermodynamic synthesis including all systems in which morphological development is possible has prompted a classification of the three known systems and certain predictions concerning a fourth group. More specific classifications (i.e. those based on habit form and crystallographic similarities) should be implicitly contained within any general thermodynamic grouping.

Before the classification is outlined it is necessary to invoke the "doctrine of infinitesimal equilibrium" otherwise known as the "principle of local equilibrium"(15). This principle states that, whatever the degree of overall metastability of a thermodynamic system, internal local equilibrium is promptly established. In particular, a volume element enclosing the interface is, to a good approximation, in a state of equilibrium according to the constitutional diagram. In any microscopic or "local" region slight temperature, pressure, and concentration gradients are necessary to drive the transformation reaction. These variations of intensive variables between adjacent atomic

positions are, however, negligibly minute when compared to the absolute value of the variables. Alternatively, the mean energy change per free path is very much less than kT.

Non-planar interfaces in unidirectionally transforming two phase systems require the establishment of a continuous spectrum of local equilibria dictated by the appropriate equilibrium constitutional diagram and controlled by interacting temperature, pressure, and concentration gradients. There must be a co-operative variation of at least two of these gradients to sustain a non-planar interface at equilibrium. This fact is used as a basis of the classification.

1 - Pure Metal Solidification - ∇T; ∇p.

This system exhibits stable non-planar interface development controlled by locally interacting temperature and pressure gradients. Figure 1 (b) illustrates a typical temperature variation with distance which may lead to non-planar growth. According to the Weinberg and Chalmers[1,2] interpretation of Figure 12, the tips of interfacial nuclei will project into the melt and will encounter progressively lower values of T_{sc}. Non-planar growth is stabilized and will continue in the presence of a negative temperature gradient in the liquid.

Kirkaldy [16] insists that if stable non-planar growth is to be possible under the above conditions there must also

exist a non-zero interfacial tension. This is because a system with a zero interfacial tension requires an invariant equilibrium interface temperature. This constraint coupled with a stable non-planar interfacial configuration will lead to a violation of the diffusion equation.

To account for the effects of interfacial tension we note that the tips of advancing projections possess small radii of curvature and high interfacial energies. There will exist associated pressure changes which result in the establishment of new equilibria along the boundary between the projection and the adjacent melt. The manifestations of these local pressure changes during phase transformations depend upon whether one or both phases are affected by the change. In the solid - liquid configurations to be considered in this section it is assumed that the pressure change associated with surface tension acts only on the solid phase.

To discuss the solidification of a pure substance we invoke the Gibbs-Duhem relations for the coexistence of two phases at equilibrium,

$$N^I d\mu^I = V^I dP^I - S^I dT_f$$
$$N^{II} d\mu^{II} = V^{II} dP^{II} - S^{II} dT_f \qquad -(6)$$

If the volumes and entropies are taken as molal quantities, then

$$N^I = N^{II} = 1 \qquad -(7)$$

Also, since the pressure on the liquid is assumed to remain con-

stant during the change in curvature of the interface

$$d\rho^{I} = 0 \qquad -(8)$$

Finally, assuming local equilibrium at the interface so that

$$d\mu^{I} = d\mu^{II} \qquad -(9)$$

then $$\frac{dT_f}{d\rho} = \frac{V^{II}}{S^{II}-S^{I}} = \frac{TV^{II}}{H^{II}-H^{I}} \qquad -(10)$$

This expression will always be negative since $H^{II}-H^{I}$ is always less than zero.

This means that, in a situation such as in Figure 1 (b), it is possible for an interfacial perturbation, with its fusion temperature lowered by surface tension, to remain in local equilibrium since the actual temperature distribution decreases towards the tip. The occurrence of stable projections can only be determined by quantitatively calculating the critical conditions necessary for non-planar growth. These conditions will be time-dependent. It is possible, however, to characterize such morphologically active systems by an interaction between temperature and pressure gradients, i.e. the symbols $\nabla T : \nabla p$. The chemical potential, being dependent, also varies along the interface.

2 - Alloy Single Crystal Growth - $\nabla T : \nabla H$, p=constant.

The solidification of alloy single crystals is accompanied by interface morphological development in the presence of appropriately arranged temperature and composition gradients. The

thermal and chemical gradients have been related in an expression (equation 5) summarizing the critical conditions for non-planar growth. Solute redistribution at the interface results in a solute rich area as indicated in Figure 9 (a). An equilibrium fusion temperature gradient results (Figure 9 (b)). When the actual temperature gradient is less than this fusion temperature gradient a constitutionally supersaturated zone exists. Non-planar interfaces may be stable in this zone since the tips of nuclei can establish local equilibria with the adjacent, higher temperature, solute poor liquid.

The analysis that has been presented [4] assumes that pressure is constant throughout the system. As was pointed out in our discussion of pure substance solidification, morphological development is accompanied by the establishment of local pressure gradients. Tiller's analysis is, therefore, only approximately true insofar as it neglects to consider the effects of pressure variations.

In summary, the development of projections during alloy single crystal growth is primarily controlled by locally interacting temperature and composition gradients. Pressure variations due to surface tension may also occur and complicate the problem of stating the conditions for local equilibrium at a non-planar interface. Ideally we classify this system by the symbols $\nabla T : \nabla H$, p=constant, bearing in mind that in actual systems P

also varies on the solid side of the interface.

3 - Widmanstätten Type Precipitation - $\nabla P : \nabla \mu_i$, T=constant.

The analysis of Widmanstätten type precipitation phenomena has called attention to the presence of interacting pressure and concentration gradients. Solute redistribution at the interface results in concentration profiles such as those indicated in Figures 6 and 7. The formation of projections with small radii of curvature is attended by local pressure changes which are felt by both the parent and precipitating phases. The equilibrium phase boundaries as determined by the constitutional diagram are shifted. New local equilibria are established between adjacent phases whose more dilute compositions are represented on Figure 5.

It is possible for an interface projection, with its equilibrium composition lowered by surface tension, to establish a new local equilibrium with the adjacent parent phase whose initial solute solubility has been decreased, since projections encounter negative concentration gradients. Widmanstätten type precipitation processes are primarily controlled by interacting pressure and composition gradients. The subsidiary condition of constant temperature is easily satisfied and simplifies analysis. Precipitation is obviously diffusion controlled and analysis is therefore complicated by the necessity of considering the time dependence of both nucleation and growth in this non-steady state

system. Although the critical conditions for precipitation are elusive the system may be classified symbolically by $\nabla P : \nabla \mu_1$, T=constant.

4 - Solid State Transformation Reactions in Ternary Systems - $\nabla \mu_1 : \nabla \mu_2$, P and T constant.

Isothermal diffusion experiments have been employed to determine constitutional diagram phase boundaries in binary systems. Unidirectional diffusion between two phases during such investigations has not, however, been observed to sustain stable non-planar interfaces. Accelerated grain boundary diffusion in polycrystalline samples is the only mechanism by which non-planar interfaces may be produced in the binary case. The pressure and composition gradients are such that metastable supersaturated zones in which favourable local equilibria could be established fail to appear. Surface tension invariably carries parts of the interface away from, rather than towards, local equilibrium.

The addition of a third component to the system just discussed adds a degree of freedom to the system. The interface between the two phases in such a ternary system, under the restrictions imposed by the principle of local equilibrium, should be capable of sustaining a stable non-planar morphology. The boundary conditions required here may be established by choosing the terminal compositions of a semi-infinite diffusion couple in such a

way that the mean diffusion-composition path crosses a two-phase region on the appropriate isothermal section of the constitution diagram at an angle to the equilibrium tie lines.

Having made a suitable choice of boundary conditions, the calculation of the diffusion path for an assumed flat interface may reveal areas of supersaturation as indicated in Figure 12. In case (a) the result could be a persistent planar interface with isolated precipitates. Case (b) could possibly result in non-isolated precipitation, i.e. a non-planar interface.

Diffusion-composition paths in ternary systems are known to be curvilinear [17] while the relative magnitude of the diffusivities of the components in such systems vary widely. It has been suggested that a path must necessarily intersect, at least once, the straight line joining the terminal composition points if mass or atoms are to be conserved [18].

In summary, it is theoretically feasible that stable non-planar interfaces may appear during solid state transformations in ternary systems provided the boundary conditions are appropriately arranged. Two interacting composition gradients may enable the establishment of local equilibria conducive to non-planar growth. Volume strain energies and surface tensions will doubtless introduce local pressure gradients which may be sufficient to modify the final configuration. For the purposes

of the classification, however, this system is typified by $\sigma\mu_1 : \sigma\mu_2$, both pressure and temperature being assumed to be constant.

Summary

The appearance of morphologically active interphase boundaries during diffusion in ternary systems would be a confirmation of the value of adopting the thermodynamic point of view in transformation problems. The classification that has been presented underlines the importance of the various controlling factors in non-planar development. It simplifies the problem by diverting attention from the mechanism of transformation and stressing the controlling influence of the three thermodynamic intensity variables; temperature, pressure, and composition. Rewriting all the classes in symbolic form results in Table 1.

It should be emphasized that the constraints imposed by the boundary conditions and the condition of local equilibrium are not usually sufficient to uniquely specify the morphology. In all cases in which morphological development appears, local equilibrium and the transport equations can equally well be satisfied by assuming a flat interface. To remove this mathematical degree of freedom variational methods must be invoked as described by Kirkaldy (19).

Class	Examples	Subsidiary Conditions	Dependent Variable
$\nabla T : \nabla P$	Pure substance solidification	none	M_1
$\nabla T : \nabla M_1$	Alloy single crystal solidification	P constant*	M_2
$\nabla P : \nabla M_1$	Widmanstätten type precipitation	T constant*	M_2
$\nabla M_1 : \nabla M_2$	Transformations in ternary diffusion couples.	P and T constant*	M_3

Table 1: The thermodynamic classification of systems capable of sustaining non-planar interface morphologies

* - conditions are approximate only.

EXPERIMENTAL

Binary and ternary diffusion couples were examined for morphological development at 500°C. in the copper-tin-zinc system and at 650°C., 1000°C., and 1800°C. in the iron-chromium-nickel system. These alloy systems were chosen because their constitutional nature appeared to be favourable for the development of non-planar morphologies.

1 - Preparation and Diffusion of Couples.

The lower melting point Cu-Sn-Zn alloys were melted in a gas-fired pot furnace using carbon crucibles. The alloys high in zinc content were prepared by fusion of a suitable amount of tin with 60% copper - 40% zinc alloy which was supplied by Anaconda Copper and Brass Company. Losses due to zinc's high vapour pressure were minimized and alloys of desired composition were obtained in this manner. All alloys were chill cast into a 1" diameter X 6" long tapered cylindrical steel mold. Subsequent heat treatment was as summarized in Table 2. A Lindberg resistance furnace with ordinary atmosphere was found to be adequate. Alloys B and D were furnace cooled because of their brittle nature.

After homogenization the ingots were sectioned with a Buehler high speed cut-off wheel into discs 1/4" in thickness and 1" in diameter. The surfaces were then wet polished on progress-

ively finer emery papers, finishing with # 600 grit. Extreme care was necessary during sectioning and polishing of brittle alloys B and D to avoid chipping and fracture.

A diffusion couple holder was constructed from a standard 1" brass pipe plumbing tee fitted with blind plugs. 3/8" copper tubing was connected to either end by 1/4" X 3/8" right angle brass fittings. This enabled the maintenance of an inert argon atmosphere within the holder at a slight excess pressure and resulted in the production of sound oxide-free welds. The holder is illustrated in Figure 13.

Couple Ni:B (see Table 2) was prepared by electroplating copper on a sample of alloy B. A standard copper sulphate - sulphuric acid bath [20] was used. Sound deposits of the order of 0.030" thick were obtained after plating for 12 hours with a current of 0.5 amperes (56 amperes per sq. ft.).

The couples were placed in the holder and allowed to diffuse in a Harrop Globar furnace. The couple temperature was continuously recorded by means of a chromel-alumel thermocouple connected to a Phillips multichannel recorder. Maximum temperature deviation was found to be 500°C. ± 3 C.°

The high melting point metals in the Fe-Cr-Ni system (see Table 3) were prepared in much the same fashion. Therefore, only details unique to this section of the work are outlined here.

Table 2:

Summary of Heat Treatment and Diffusion Data for the Cu-Sn-Zn System.

Couple	Alloy	Nominal Composition	Homogenization			Diffusion	
			Temp. (°C.)	Time (hrs.)	Cooling Rate	Time at 500°C.(hrs.)	Cooling Rate
A:B(1)	A	Cu-15%Sn	750 500	120 48	water quenched	24	50°C./min.
	B	Cu-15%Sn-35%Zn	700 500	120 48	furnace cooled		
A:B(2)	"	"	"	"	"	48	"
A:B(3)	"	"	"	"	"	120	"
C:D(1)	C	Cu-35%Zn	850 500	120 48	water quenched	24	"
	D	Cu-32.5%Sn	700 500	120 48	furnace cooled		
E:B(1)	E	100%Cu	electroplated			24	water quenched
	B	(as above)	(as above)				
E:B(2)	"	"	"			48	50°C./min.
E:B(3)	"	"	"			120	"
A:D(1)	A	(as above)	(as above)			120	"
	D	"	"				

Couple M:N was prepared by electroplating chromium on 1/16" cold-rolled electrolytic nickel sheet in a standard high temperature chromic acid - sulphuric acid bath. (20) Plating for 24 hours at a current density of approximately 200 amperes per sq. ft. resulted in sound adherent deposits 0.010" to 0.020" thick. The samples were sectioned and placed directly in to the Harrop Globar furnace, maintained at 1300°C., for the required time interval and water quenched to room temperature. The furnace temperature was verified using a Pyro Micro-Optical optical pyrometer and found to be within 10 C.° of 1300°C. at all times.

Couple O:P was prepared by electroplating a sample of 18% Cr - 8% Ni stainless steel with a thick layer of pure iron. The couple was placed directly in the Harrop furnace and diffused at 650°C.±2 C.° Diffusion was terminated by water quenching the sample to room temperature.

The alloys for the other couples were prepared by induction melting in a Tocco air melt unit using a zirconium crucible fitted with a magnesia lid. Argon was admitted via this lid. Clean oxide-free melts were produced and chill cast into the tapered steel mold.

After homogenizing, sectioning and polishing the couples were mounted in a composite mild steel - stainless steel holder. This holder, illustrated in Figure 14, was then

Table 3:

Summary of Heat Treatment and Diffusion Data for the Fe-Cr-Ni

Couple	Alloy	Nominal Composition	Homogenization		Diffusion		
			Temp (°C)	Time (hrs)	Temp (°C)	Time	Cooling Rate
M:N(1)	M	100% Cr	electroplated		1300	5 minutes	water quenched
	N	100% Ni	cold rolled sheet				
M:N(2)	"	"	"		"	15 minutes	"
M:N(3)	"	"	"		"	30 minutes	"
O:P(1)	O	100% Fe	electroplated		650	24 hours	"
	P	Fe-16%Cr-8%Ni	commercial alloy				
Q:N(1)	Q	Fe-13%Cr	1300 1000	120 48	1000	"	30°C/minute
	N	100% Ni	cold rolled sheet				

enclosed in a welded gas-tight Inconel enclosure (see Figure 15). The assembled apparatus was then placed in the Harrop Globar furnace and diffused at 1000°C. ± 5 C.° for 24 hours in an argon atmosphere and allowed to furnace cool. The cooling rate was estimated to be 50°C. per minute.

2 - Metallographic Examination of Diffusion Couple Interfaces:

All couples were sectioned and mounted for metallographic examination in Buehler "Transoptic" mold material as in Figure 16. Standard procedure was employed in wet grinding with emery paper to # 600 grit.

The polishing procedure employed throughout consisted of final polishing using # 1551 AB α-alumina # 2 in conjunction with # 1570 AB Duracloth supplied by Buehler Limited. In some instances the above procedure was followed by a further polishing employing # 1552 AB γ- alumina. A slurry polishing technique was developed especially for the brittle Cu-Sn-Zn couples. A 1" wide fluid-tight rubber retainer was fixed to the perimeter of the polishing wheel. A pool of suspended alumina was thereby maintained in contact with the sample throughout the polishing cycle.

The sample mounting material was drilled as in Figure 16 to enable the sample to rotate while pivoting on a specially constructed sample holder. This holder is illustrated in

Figure 17. If the pressure between the sample and the wheel, which was made to rotate at approximately 30 revolutions per minute, was properly regulated the difference in relative velocity along the radius of the polishing wheel caused the sample to rotate about its pivot at between 60 to 80 revolutions per minute.

This semiautomatic polishing apparatus enabled the imposition of a steady light pressure between the sample and the polishing wheel. The suspended alumina slurry is agitated by the rotating motion of the sample while the wheel acts as a centrifuge and causes unwanted coarse particles to separate at the perimeter of the wheel. A high quality scratch-free surface was easily obtained with this apparatus.

The pH of the alumina slurry was maintained at 7 by the addition a small quantity of dilute acid or base as required. The tendency of couples to establish an electrochemical cell and preferentially etch or corrode while in contact with the aqueous slurry for extended periods of time was thereby eliminated. Polishing times varied within the range 5 to 20 minutes depending upon the hardness and surface area of the sample.

8 - Electron Probe Microanalysis of Diffusion Couples [21]:

The morphological nature of the phase interfaces in couples E (100%Cu):B (60%Cu-35%Zn-15%Sn) and Q (100%Ni):M (87%Fe-13%Cr) prompted a quantitative determination of their actual diffusion-composition paths by means of an electron probe microanalyser. An "Intec Cameca" probe at the International Nickel Company Research Laboratories in Bayonne, New Jersey, U. S. A. was used for this work.

An electron probe is essentially a fine focus x-ray tube in which the specimen is the target. A beam of 10-50 Kev electrons with a focal spot approximately 1 micron in diameter makes possible the accurate measurement of the compositions and composition gradients of a large number of elements in and around small precipitate particles. The spot size limits the beam current to the order of one microampere. Electrons of the energies used, 50 Kev, penetrate the surface approximately two microns. Electron excitation gives rise to excitation intensities 200-1000 times greater than fluorescent x-ray excitation. An emission count of 10 c.p.s. above a background count of 50 c.p.s. is the limit of resolution. Pure metals yield emission counts of the order of 10,000 c.p.s. The limit of detectability is therefore 0.1% composition or less.

Specimens may be moved about to bring any desired area into position for analysis. Point-to-point scans may be made by manually moving the specimen with respect to the beam. Each point analysis requires radiation and counting for each element for approximately 50 seconds. An optical microscope system makes possible direct location and observation of the area being analysed.

Provision has been made for continuous scanning along a predetermined path up to 150 microns in length. During continuous scanning the counter signal is recorded on an oscilloscope. The signal trace is photographed directly by a time exposure with a Polaroid camera using negative film.

Specimens for this work, 1/4" x 1/4" x 5/16", were prepared and mounted in a special plastic holder for polishing. The holder is illustrated in Figure 16. Polishing procedure was as previously outlined. Polishing time was kept to a minimum to avoid undesirable surface relief. A light chemical etch was employed to aid in optical viewing.

Analysis of 100%Cu: Cu-35%Zn-15%Sn Diffusion Couple:

Figure 31 represents the area that was examined. Three individual continuous scans were taken along the line shown on the micrograph. The electron beam produced a dark line apparently due to interaction between the electron beam and the carbon that was

purposely deposited on the surface after it was found that this sample possessed poor conductivity. The sample acted as a capacitor and caused erratic wandering of the electron beam. The negatives obtained were projected on appropriately arranged graph paper. These enlarged traces are included as Figures 18, 19, and 20. It is evident from these graphs that the relative positions of the interfaces traversed vary from scan to scan. This is attributed to unavoidable differences in scanning rates, scanning paths, and terminal positions. Figure 21 graphically represents composition variation with distance before correction for these differences. Considerable error is evident here when the three curves are summed.

Copper and zinc, being adjacent on the periodic scale, form and ideal pair for quantitative analysis since they possess almost identical absorption and enhancement coefficients if no other elements are present. Tin and zinc are a considerably less ideal pair, however, since tin radiation causes zinc to radiate simultaneously. Since the tin scan results are obviously in error they were discarded. The absence of detectable amounts of tin in the α-brass needle suggested that a correction factor of 0.957 should be applied to the copper and zinc results. After applying this correction and assigning the end point values as determined by chemical analysis of the γ-phase the tin curve was determined by difference. Figure 22 summarizes the best estimates that can

be made of composition variations with distance consistent with the data from the phase diagram, the chemical analysis, and the electron probe microanalysis.

Figure 23 is the 500°C. isotherm plotted in terms of atomic percentages. The estimated diffusion-composition path for needle-like sections of the interface is represented on this isotherm along with a hypothetical path for the same couple when there is no morphological development.

Analysis of 100%Ni:Fe-18%Cr Diffusion Couple:

It was not found necessary to evaporate carbon on the surface of this sample. The micrograph in Figure 33 illustrates the path chosen.

In this case a point-to-point scan of nickel content, a point-to-point check of chromium content, and continuous scans of iron, nickel, and chromium composition variations with distance were performed.

Figures 24, 25, and 26 represent the enlarged oscilloscope traces obtained. Figure 27 presents the corrected data as a function of distance while Figure 28 is the estimated diffusion-composition path superimposed on the appropriate 1000°C isotherm.

RESULTS AND DISCUSSION

The Cu-Sn-Zn and Cr-Fe-Ni systems were studied here because their constitutional natures appeared to be conducive to the production of non-planar morphologies within the boundary conditions of a diffusion couple. The Cu-Sn-Zn 500°C. isotherm [22] contains an extensive two-phase region separating the α and γ (or δ) single-phase regions. Terminal compositions at opposite corners of the two-phase field may be selected such that the mean composition-diffusion path is non-parallel to the equilibrium tie lines. The 650°C. isotherm of the Cr-Fe-Ni ternary system [23,24] consists, in part, of a suitable two-phase $\alpha+\gamma$ region between the single-phase regions near the iron-rich corner of the diagram. The 1000°C. isotherm of this system [23,24] possesses an extensive $\alpha+\gamma$ region and was also thought to be appropriate to the experimental purposes.

As examples of binary diffusion systems, couples were chosen at 500°C. in the Cu-Sn system and 1200°C. in the Cr-Ni system.

After diffusion and metallographic preparation the interfaces of the couples (see Tables 2 and 3) were examined microscopically for morphological development. Micrographs and discussions of all couples that were observed to exhibit interesting features are presented in this section.

Couple A:B - Cu-15%Sn:Cu-15%Sn-33%Zn - 500°C.

Figure 20 includes a micrograph which is typical of the interface of this group of couples. The cuspoidal $\alpha+\gamma$ interface, the γ- phase idiomorphs, and the porosity in the $\alpha+\gamma$ region are features peculiar to these diffusion systems.

The cusps at the interface are due to preferential grain boundary diffusion and have no bearing on the morphological problem considered here. This section of the interface can therefore be regarded as substantially planar. The precipitation of γ-brass in the α-bronze to form a two-phase region suggests that the composition-diffusion path is qualitatively of the form illustrated in Figure 23. Part of the $\alpha+\gamma$ region of the isotherm was traversed by the diffusion path so that a zone of supersaturation was established wherein nucleation and growth of γ became possible. A volume change during the $\alpha\rightarrow\gamma$ transformation may be responsible for the extensive porosity.

These particular boundary conditions result in the establishment of a constitutionally supersaturated zone similar to that discussed in the theory and schematically illustrated in Figure 12(a). A persistent planar interface with morphologically active isolated precipitates appears in such a system.

Couple C:D - Cu-35%Zn:Cu-3%.5%Sn - 500°C.

A micrograph of the interface region and a diagram of the postulated composition-diffusion path traversed are included in Figure 30. No stable morphological development was observed at the interfaces of these couples. This diffusion system differs from the other two systems reported in the Cu-Sn-Zn group in that the extent of advance of the $\alpha+\gamma$ interface with respect to the original weld is much smaller.

Since neither a morphologically active interface nor an isolated precipitate appeared in this case it was decided that attention should be returned to systems similar in nature to couple A:B. One terminal composition was changed in an attempt to eliminate the phenomena of isolated precipitation and to produce a stable non-planar morphology at the $\alpha+\gamma$ interface. The result of this change was couple E:B.

Couple E:E - 100% Cu: Cu-15%Sn-35%Zn - 500°C.

Figures 31 and 32 include micrographs of interface regions representative of this diffusion system. The Cu-δ interface is basically cuspoidal and similar to that generated in couple A:B. Associated with this interface are a large number of Widmanstätten type needles and grain boundary and intergranular idiomorphs of α- brass. Metallographic examination has revealed that the α needles, which are rods cylindrical or lens-like in shape and which continuously decrease in cross-

section, are continuous with the cuspoidal α-brass interface and terminate in sharp points in the γ-brass. This would seem to suggest that growth of the tips of these needles is accompanied and perhaps controlled by significant local pressure changes. These pressure gradients may be established by the surface tension associated with the small radius of curvature of the tip and/or a volume change during the $\gamma \rightarrow \alpha$ transformation.

The composition-diffusion path, quantitatively estimated by an electron probe microanalysis, is of the form illustrated in Figures 23 and 32. The best estimate of a composition-diffusion path that is consistent with the equilibrium constitutional relations, the electron-probe data, and the terminal compositions is that shown on the 500°C. isotherm that is Figure 23. This data was obtained in an attempt to detect the presence of zones of supersaturation in the interface region and to differentiate between the composition-diffusion paths for the needle and cusp-like interfaces. The data obtained, however, is not of sufficient accuracy.

By modifying the boundary conditions of couple A:B the zone of isolated precipitation has been eliminated. Conditions now appear to favour a composition-diffusion path similar in nature to that outlined previously in the theory section and schematically represented in Figure 12(b). A morphologically active $\alpha \rightarrow \gamma$ interface has been produced. The terminal com-

positions are such that, under the restrictions of local equilibrium, a stable non-planar morphology is possible.

The precipitation of α-phase from supersaturated γ-phase may occur at grain boundaries, at intergranular sites, and at the original α-phase boundary. In this particular case, all three nucleation sites appear to be active.

The needle-like precipitate closely resembles the Widmanstätten type configuration suggesting that local pressure increases due to surface tension and volume change are present. It would follow that the formation of α-phase needles and idiomorphs occurs under the controlling influence of two interacting chemical potential gradients and that pressure may, in fact, locally vary and in some way control the degree and kind of precipitation observed. However, to the first approximation, the classification of this system as controlled by two interacting chemical gradients, $\nabla\mu_1 : \nabla\mu_2$, is valid.

Couple A:D - 100%Cu: Cu-32.5%Sn - 500°C.

The interface structure was observed to be planar. The remarks made concerning couple C:D apply here also. No micrograph is included.

Couple M:N - 100%Cr: 100%Ni - 1300°C.

This system was examined metallographically and found to exhibit no indication of being capable of sustaining stable non-planar interfaces. This substantiates the predictions

made concerning binary system couples. No micrographs are included.

Couple O:P - 100%Fe: Fe-18%Cr-8%Ni - 650°C.

The phase transformation boundary propagation distance was observed to be small and the interface remained essentially planar. It is quite possible that such diffusion systems, allowed to diffuse for much longer intervals of time, are morphologically active. Rather than pursue this question, the Fe-Cr-Ni ternary system was explored at higher temperature as follows.

Couple Q:N - Fe-13%Cr: 100%Ni - 1000°C.

Micrographs of the interface in this diffusion system are included in Figures 33 and 34. The morphological nature of the interface has apparently been changed during cooling from the diffusion temperature by the appearance of minute projections. A martensitic type of transformation substructure appears throughout the Fe-13%Cr phase.

The electron probe microanalysis determination of the composition-diffusion path is summarized in Figures 28 and 34 and seems to suggest that no morphological development should occur in this system.

SUMMARY

This thesis has examined the present state of knowledge concerning interface form during solid - liquid and solid - solid transformation reactions. A thermodynamic approach has called attention to the various ways in which interacting thermodynamic intensive variables control interface morphological development. A classification of transforming systems into four distinct groups based on the principle of local equilibrium has been outlined.

Liquid - solid transformations in one and two component systems and solid - solid Widmanstätten type transformations in two component systems appear to be controlled by interacting temperature and pressure gradients, temperature and composition gradients, and pressure and composition gradients respectively. Solid - solid transformation reactions in three component diffusion couples was predicted to be capable of sustaining stable non-planar interfaces in some cases. This fourth group is controlled primarily by interacting composition gradients.

Experimentally, a search has been made for the boundary conditions required to produce stable non-planar morphologies in ternary diffusion couples. The occurrence of needle-like interface morphologies in a unidirectionally transforming couple in the Cu-Sn-Zn system has been noted. A similar search in the system Cr-Fe-Ni was unsuccessful.

It has been shown thermodynamically and experimentally that it is possible to produce constitutionally supersaturated regions in unidirectionally transforming ternary system diffusion couples. Supersaturation can result in either isolated precipitates or stable non-planar interfaces. Attempts to quantitatively determine composition-diffusion paths and the presence of constitutionally supersaturated regions were unsuccessful mainly because of the limited accuracy of the electron probe microanalysis data.

REFERENCES

1. Weinberg, F. and Chalmers, B., Canadian Journal of Physics, 29, 382-92, (1951).
2. Weinberg, F. and Chalmers, B., Canadian Journal of Physics, 30, 488, (1952).
3. Rutter, J. W. and Chalmers, B., Canadian Journal of Physics, 31, 15, (1953).
4. Tiller, W. A., "Growth and Perfection of Crystals", (John Wiley and Sons, Inc., New York), 1958, 332-41.
5. Tammann, G., "State of Aggregations", (D. Van Nostrand Co., New York), 1925.
6. Stranski, I. N., Disc. Faraday Society, 5, 15, (1949).
7. Frank, C. F., Disc. Faraday Society, 5, 48, (1949).
8. Chalmers, B. and Martius, U. M., Phil. Mag., 43, 686, (1952).
9. Dubé, C. A., Doctorate Thesis, Carnegie Institute of Technology, (1948).
10. Dubé, C. A., Rev. de Met., 55, 201-210, (1958).
11. Aaronson, H. I., "Precipitate Morphology", private communication, 1960.
12. Heckel, R. W., and Paxton, H. W., "The Growth of Procutectoid Cementite in Steels", (Interim report #1, Carnegie Institute of Technology, Pittsburgh), 1959.
13. Zener, C., Trans. AIME, 167, 550, (1946).

14. Hillert, M., Jernkont. Ann., 141, 757-89, (1962).

15. Prigogine, I., "Thermodynamics of Irreversible Processes", (Charles C. Thomas - Publisher), 1955, 17.

16. Kirkaldy, J. S., private communication, 1961.

17. Clark, J. B., and Rhines, F. N., Trans. ASM, 51, 199-217, (1959).

18. Meijering, J. L., Discussion of Clark and Rhines' paper.

19. Kirkaldy, J. S., "Theory of Diffusional Growth in Solid - Solid Transformations", Symposium on the Decomposition of Austenite by Nucleation and Diffusional Growth, (to be published by Interscience Publishers, New York).

20. Gray, A. G., "Modern Electroplating", (John Wiley & Sons, New York), 1953.

21. Birks, L. S., "X-ray Spectrochemical Analysis", (Interscience Publishers, New York), 1959.

22. Smithells, C. J., "Metals Reference Book", (Butterworths Scientific Publications, London), 1955, p 516.

23. As above, p 505.

24. Pugh, J. W., and Nisbet, J. D., Trans. AIME, 188, 268, (1950).

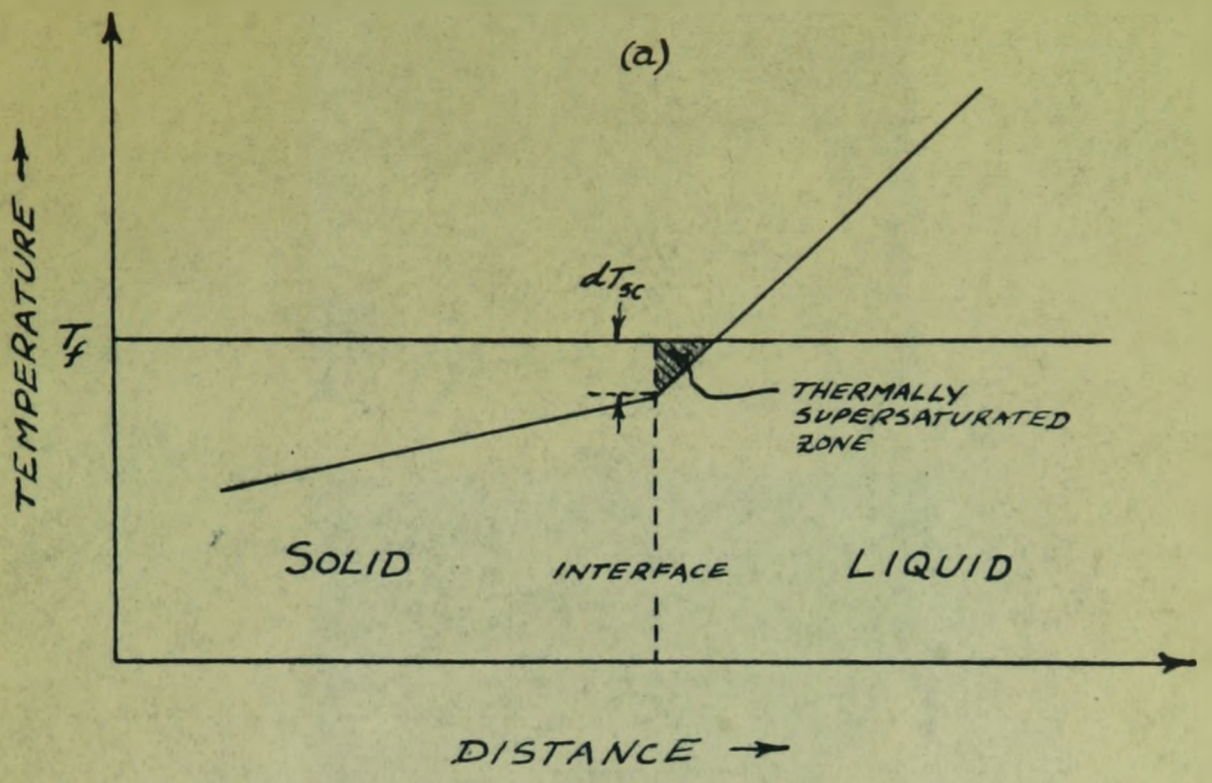

Figure 1: Temperature variation with distance at a solid - liquid interface during (a) unidirectional heat flow[1] and (b) lateral heat flow through the melt and conduction of heat through the solid[2].

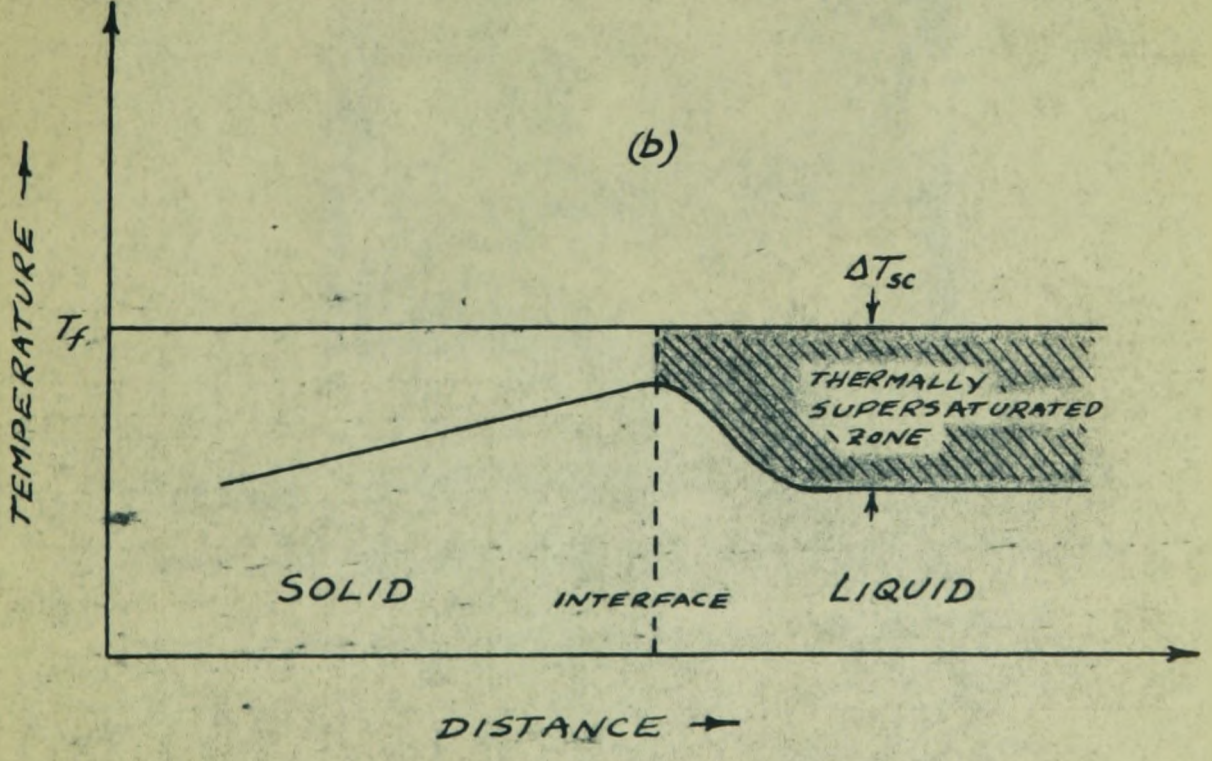

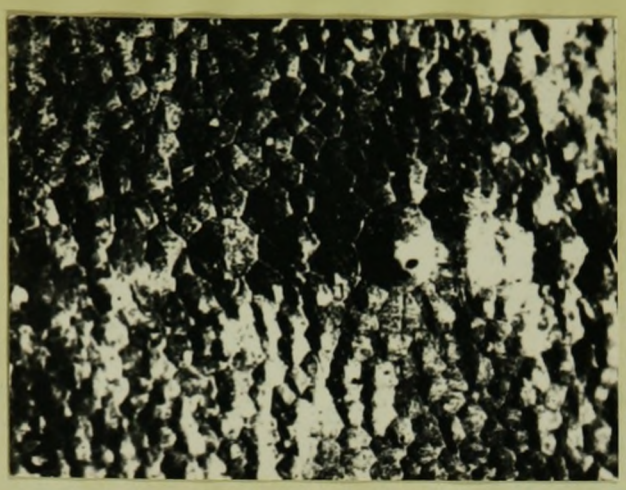

(a)

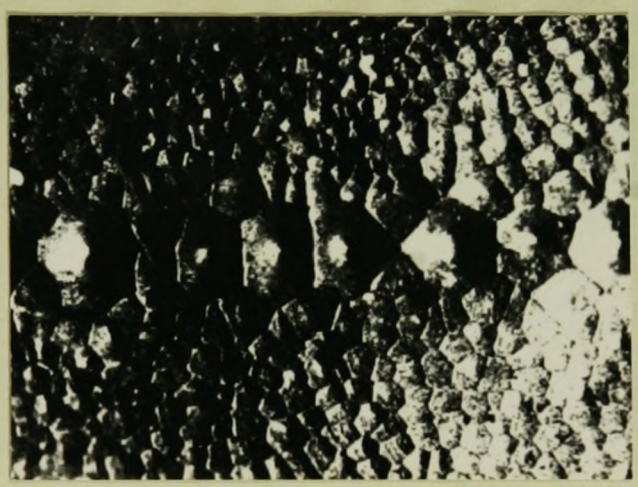

(b)

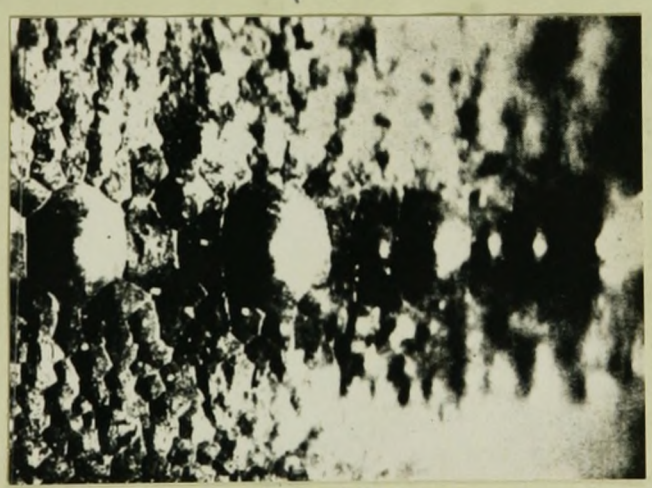

(c)

Figure 2: Decanted solid - liquid interface of pure lead showing cellular development. Growth time increases from (a) to (c). X 50 [2,3].

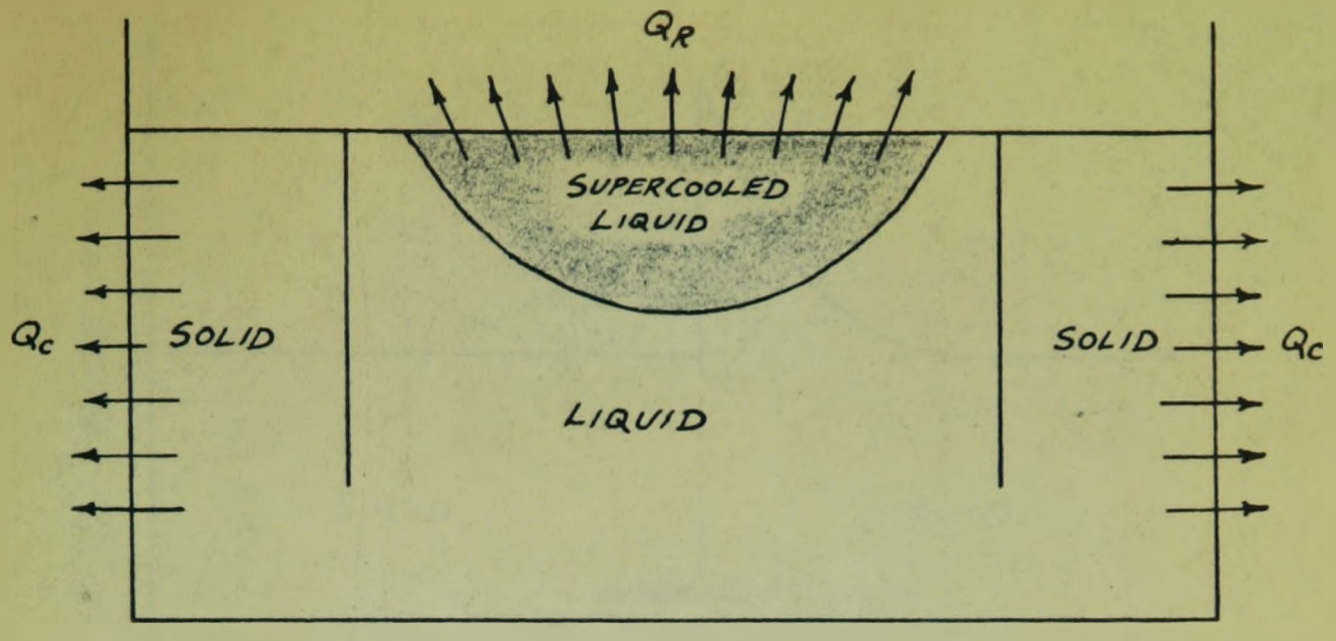

Figure 3: Supercooling of a pure melt due to surface radiation of heat to the atmosphere.

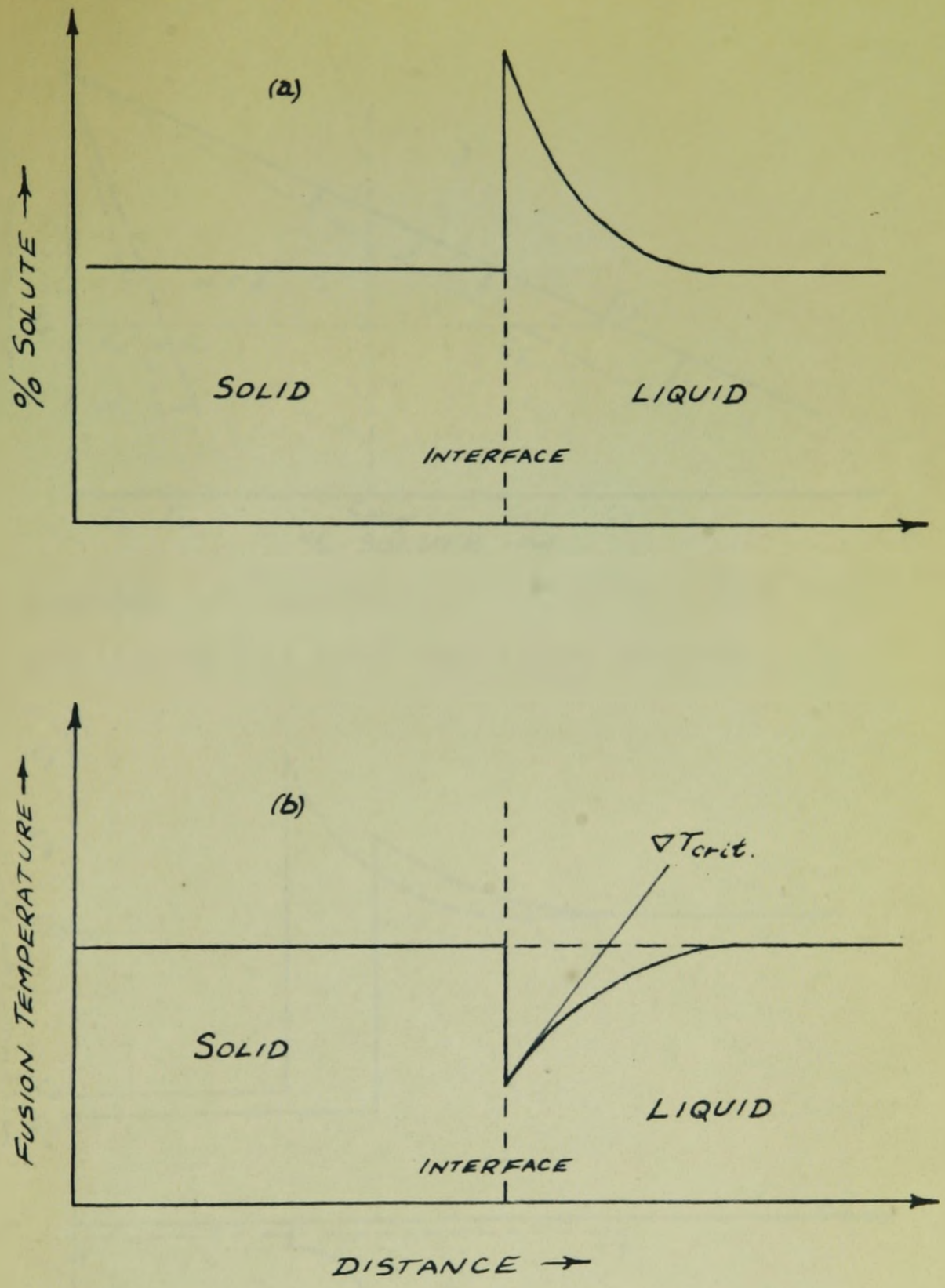

Figure 4: The variation with distance of (a) solute concentration[4] and (b) equilibrium fusion temperature at an advancing solid - liquid interface.

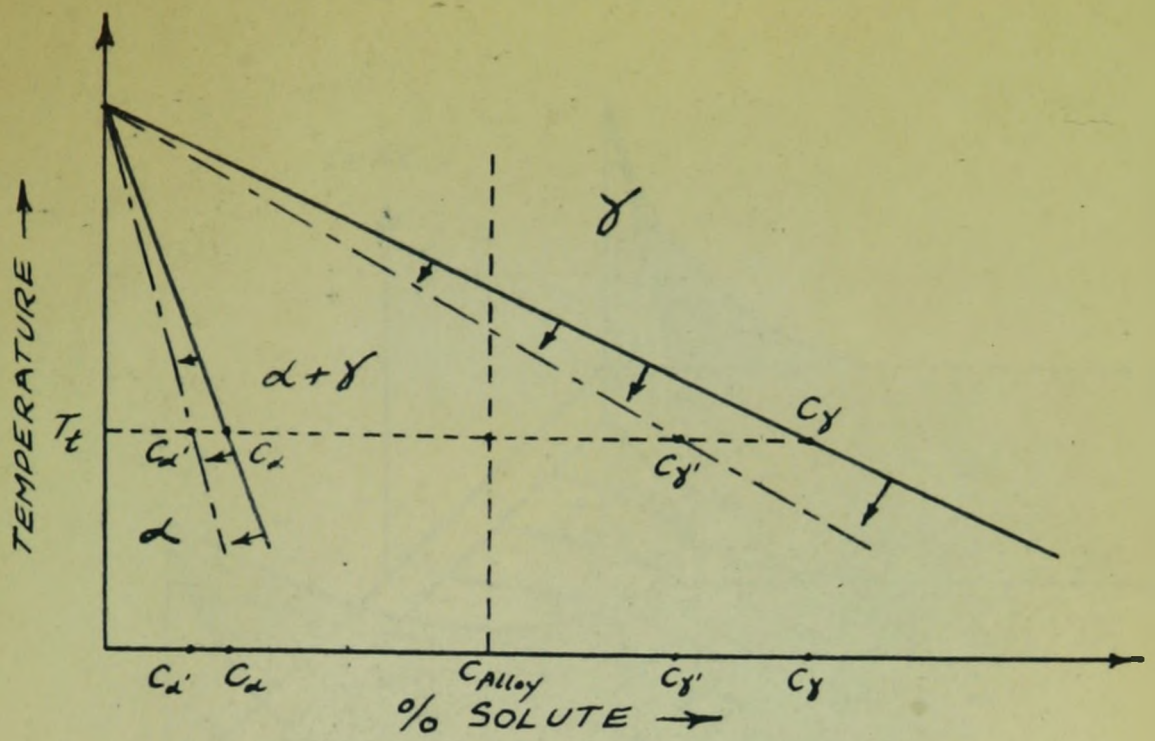

Figure 5: The decrease in equilibrium solute solubility due to a local increase in pressure.

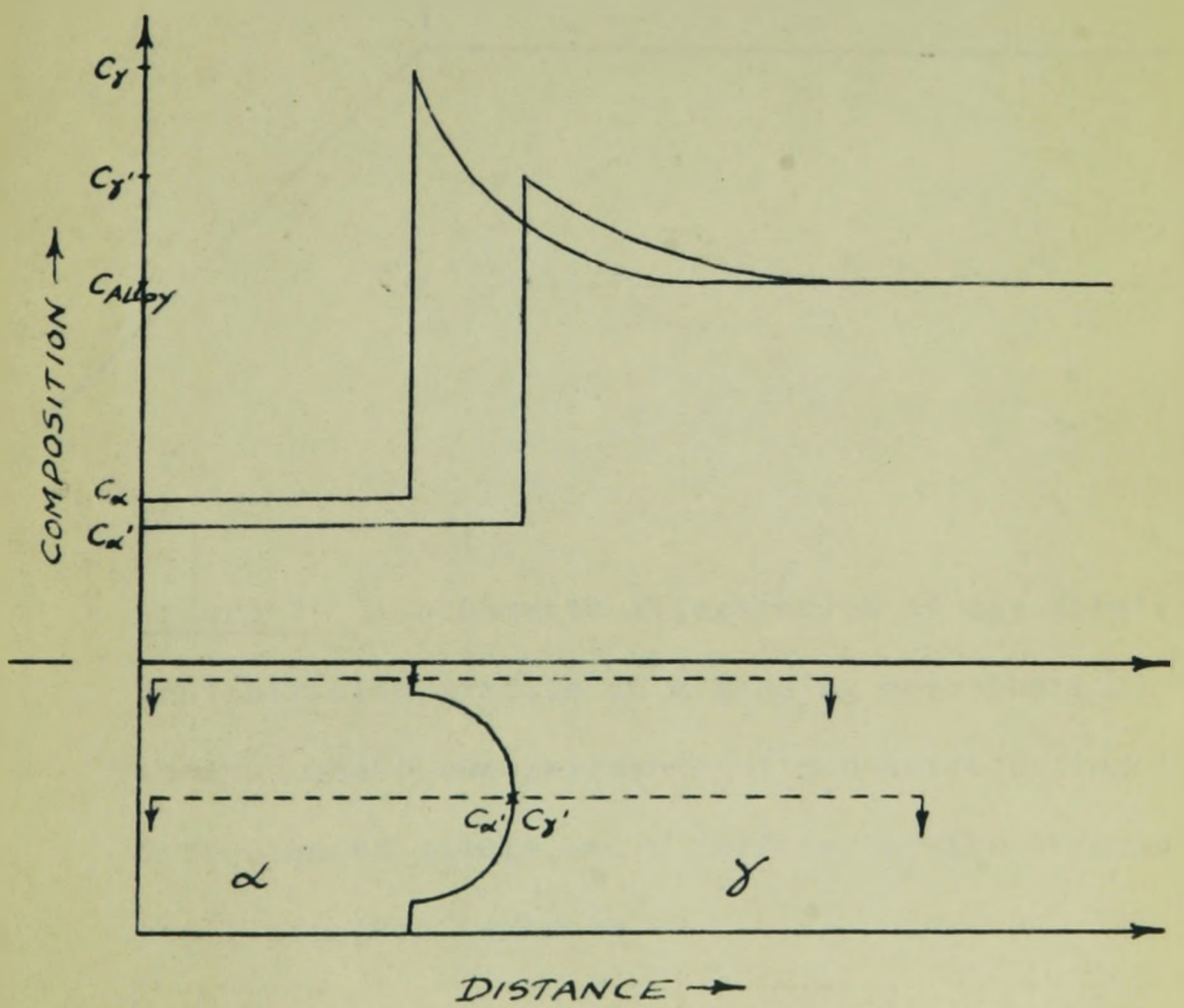

Figure 6: Solute redistribution profiles during Widmanstätten type precipitation.

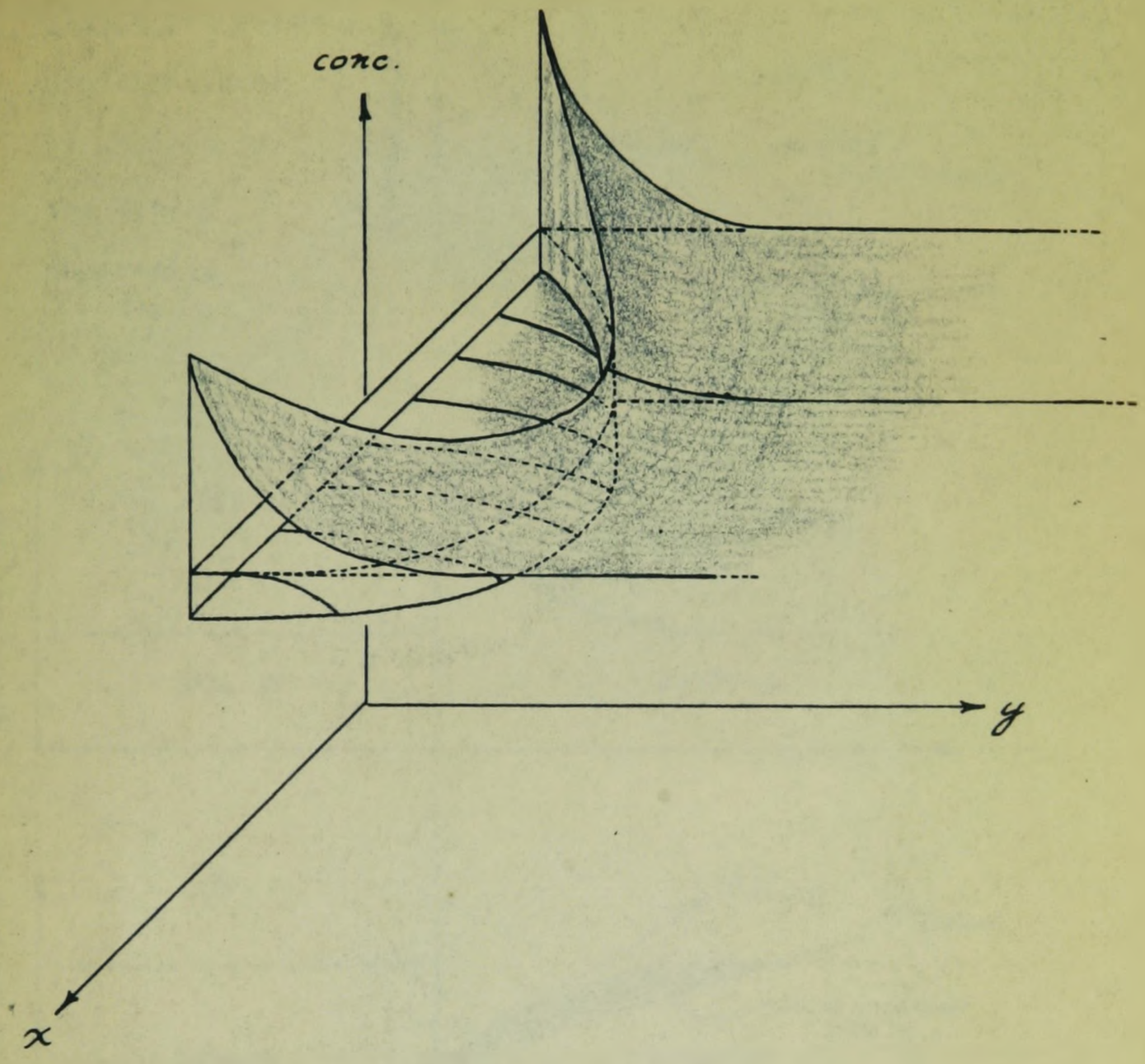

Figure 7: A schematic illustration of the solute concentration profile of a growing hemispherical nucleus under the influence of non-unidirectional diffusion of solute and a surface tension induced local pressure increase.

Figure 8: Alloy constitutional parameters for the Tiller derivation.

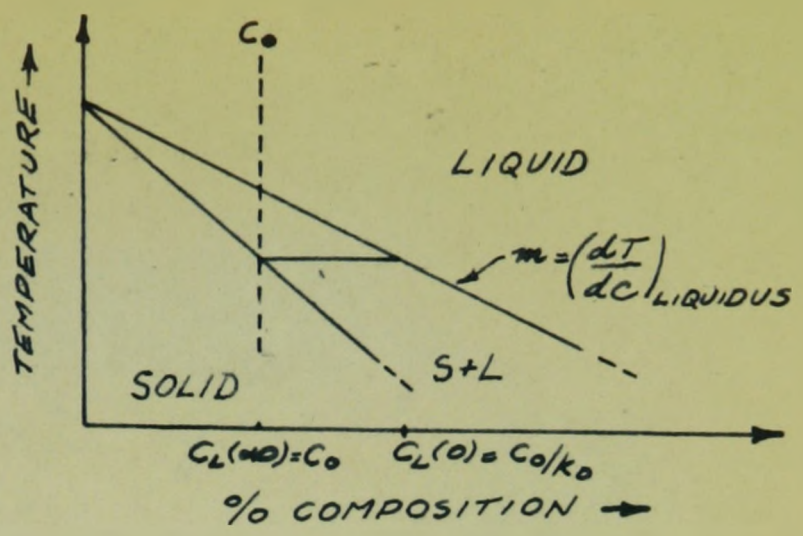

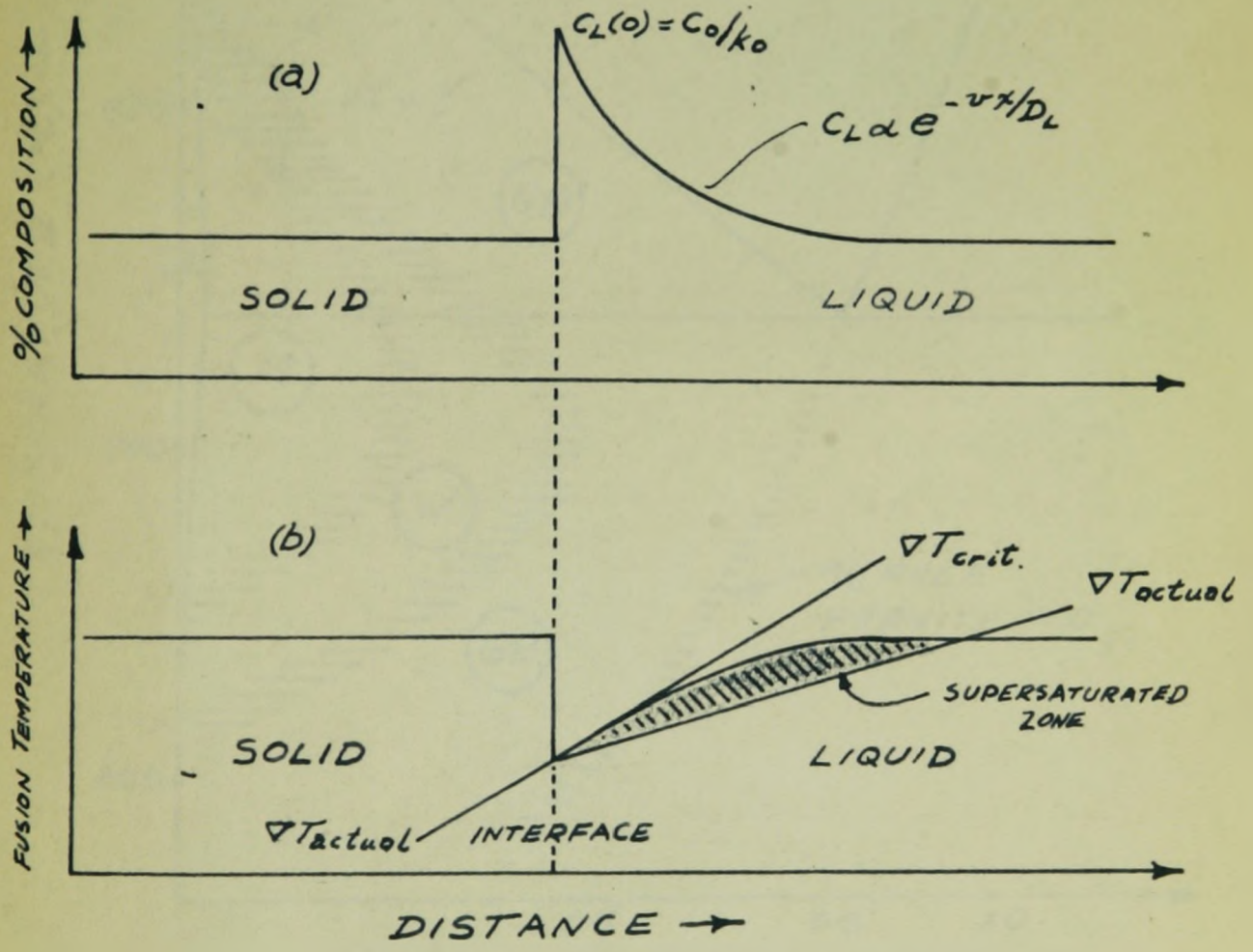

Figure 9: The variation with distance of (a) solute concentration and (b) equilibrium fusion temperature near the interface during steady state solidification of a binary alloy[4]. ∇T_{actual} necessary for stable non-planar growth is shown in (b).

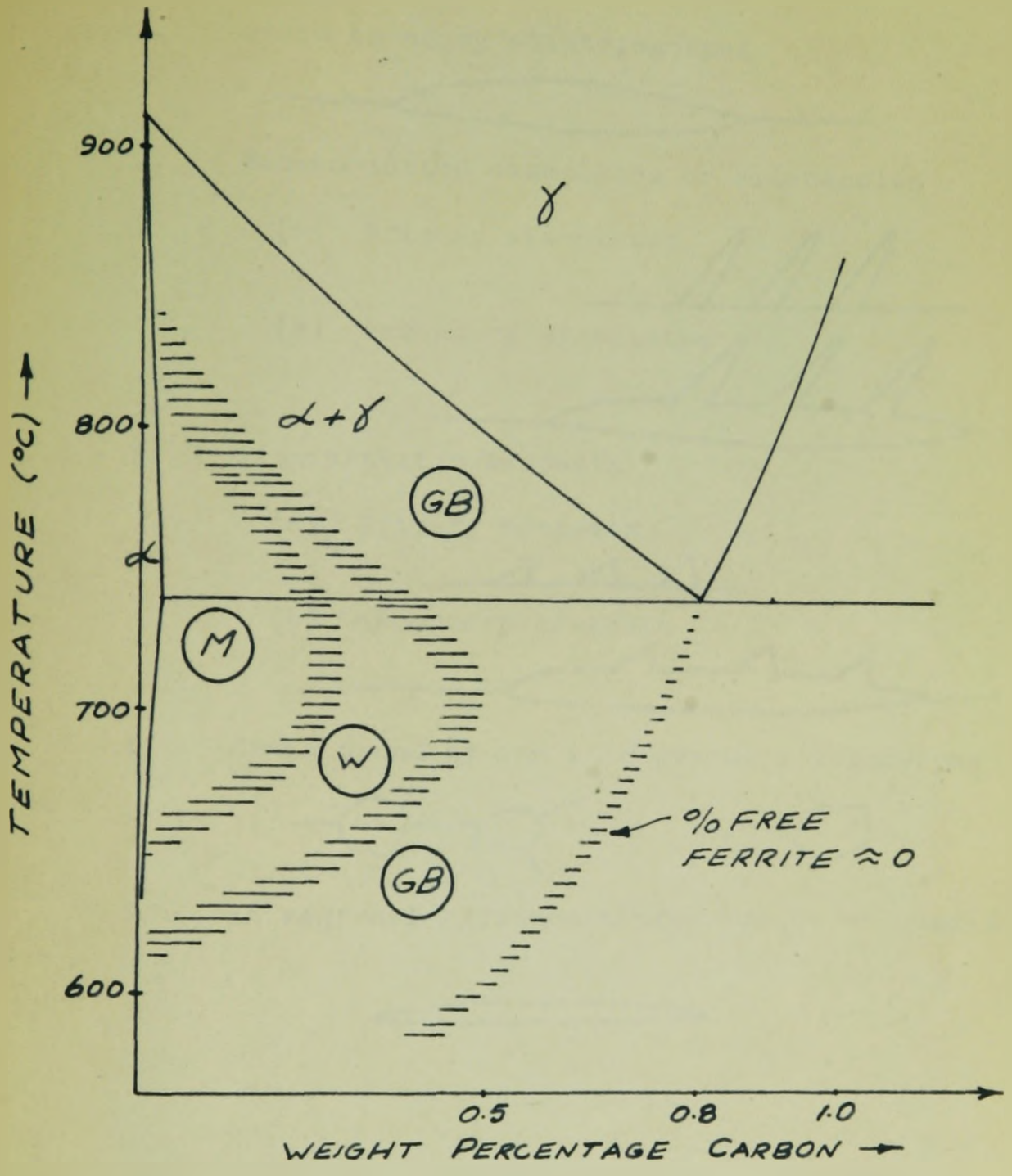

Figure 10: Microstructure as a function of temperature and carbon content for a commercial steel of grain size ASTM 0 to 1[10].

Figure 11: The Dubé Morphological Classification

1. Grain boundary allotriomorphs

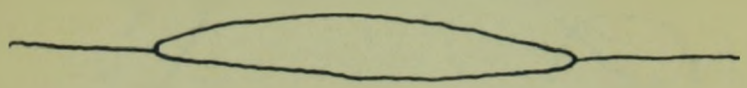

2. Widmanstätten sideplates or sideneedles

(a) Primary sideplates

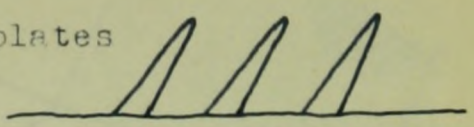

(b) Secondary sideplates

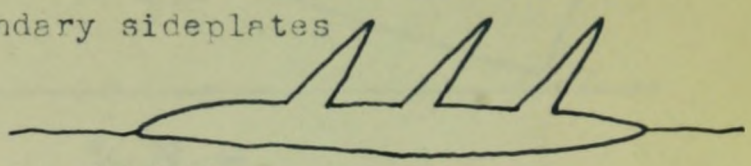

3. Widmanstätten sawteeth

(a) Primary sawteeth

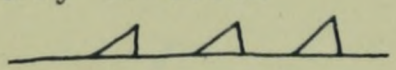

(b) Secondary sawteeth

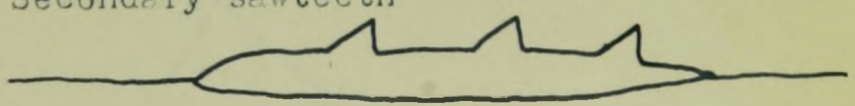

4. Grain boundary and intragranular idiomorphs

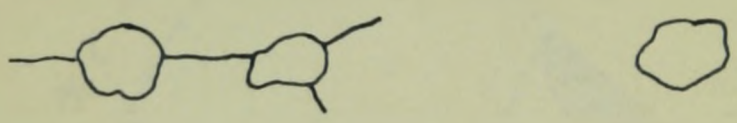

5. Intragranular Widmanstätten plates or needles

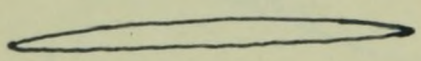

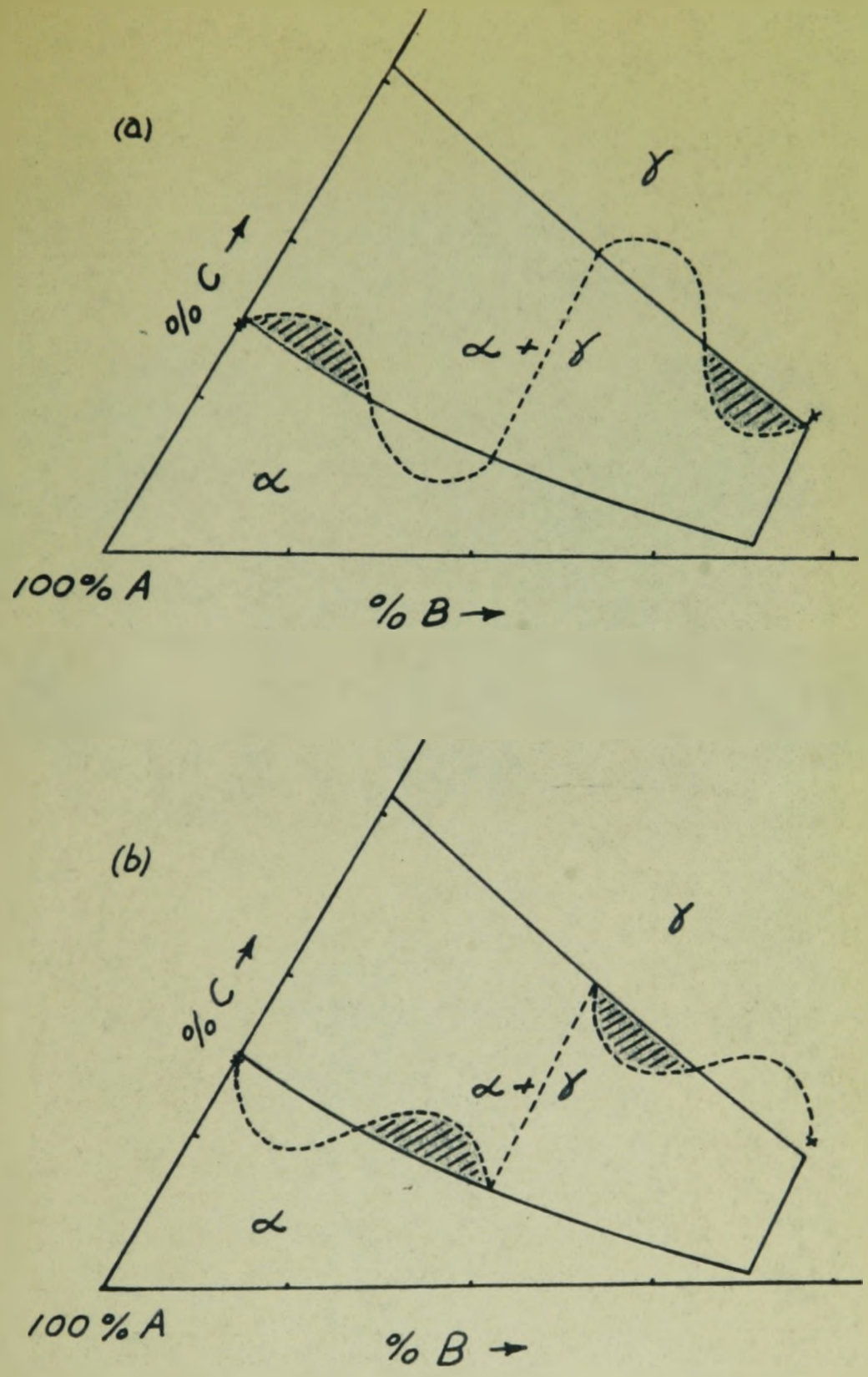

Figure 12: Constitutionally supersaturated regions produced during diffusion in a ternary system.

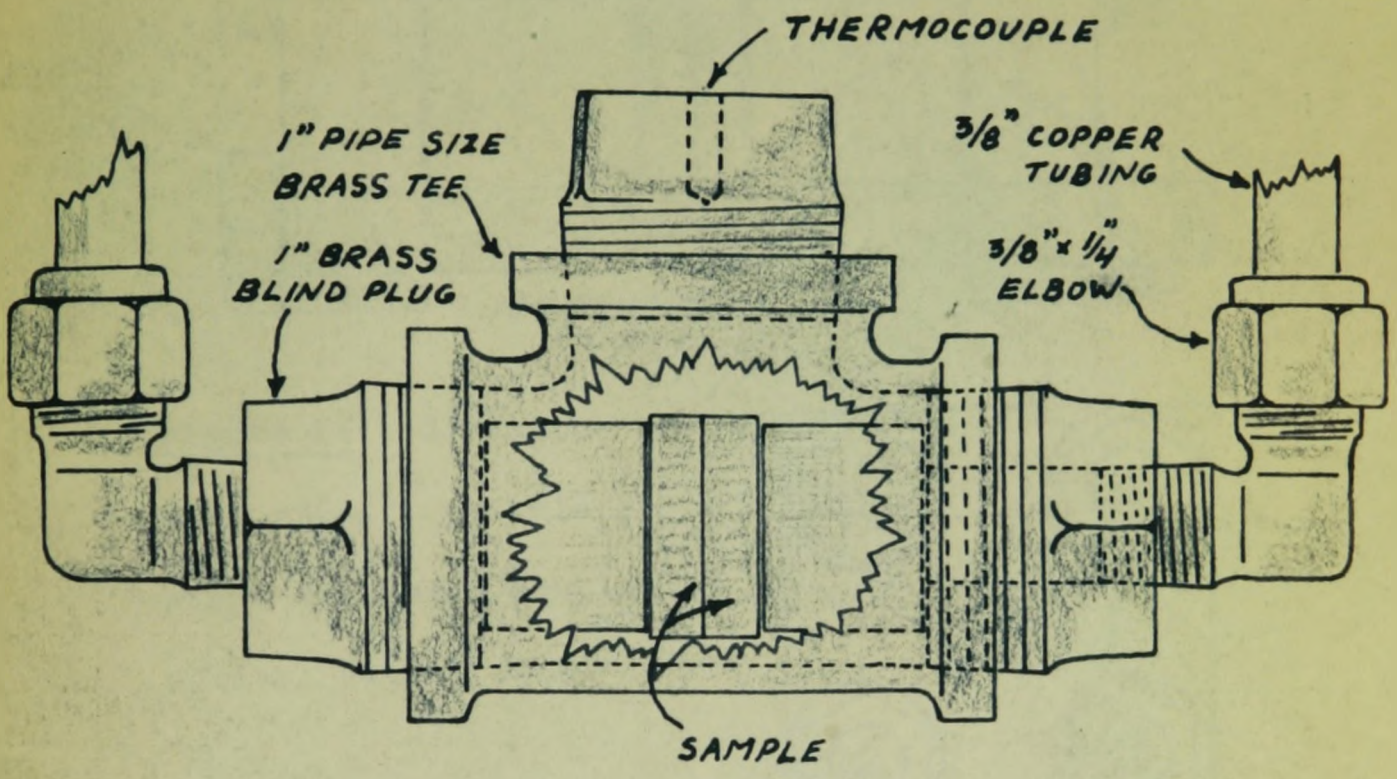

Figure 13: Holder for Cu-Sn-Zn diffusion couples. Actual size.

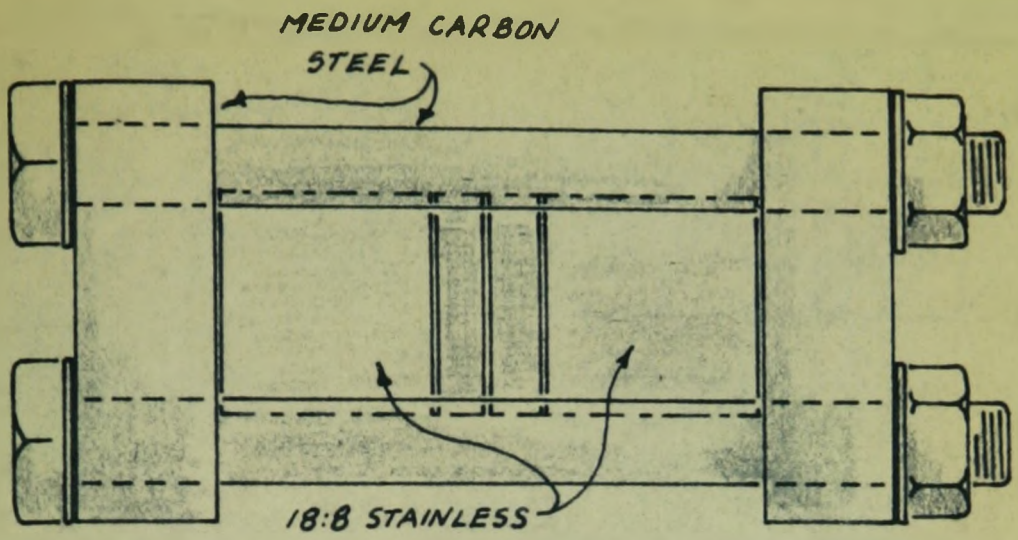

Figure 14: Composite mild steel - stainless steel diffusion couple holder, actual size.

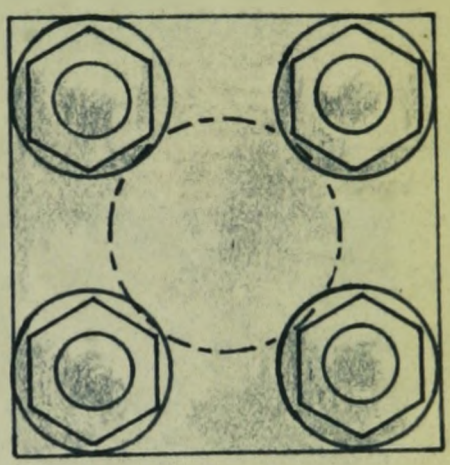

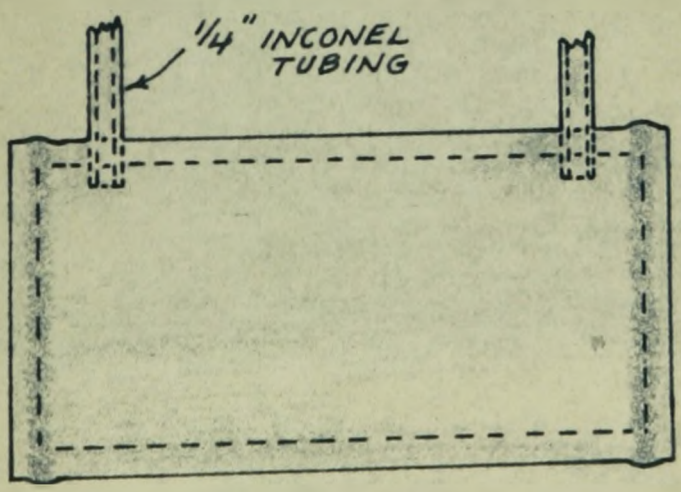

Figure 15: Gas-tight welded Inconel diffusion couple and holder container, ½ actual size.

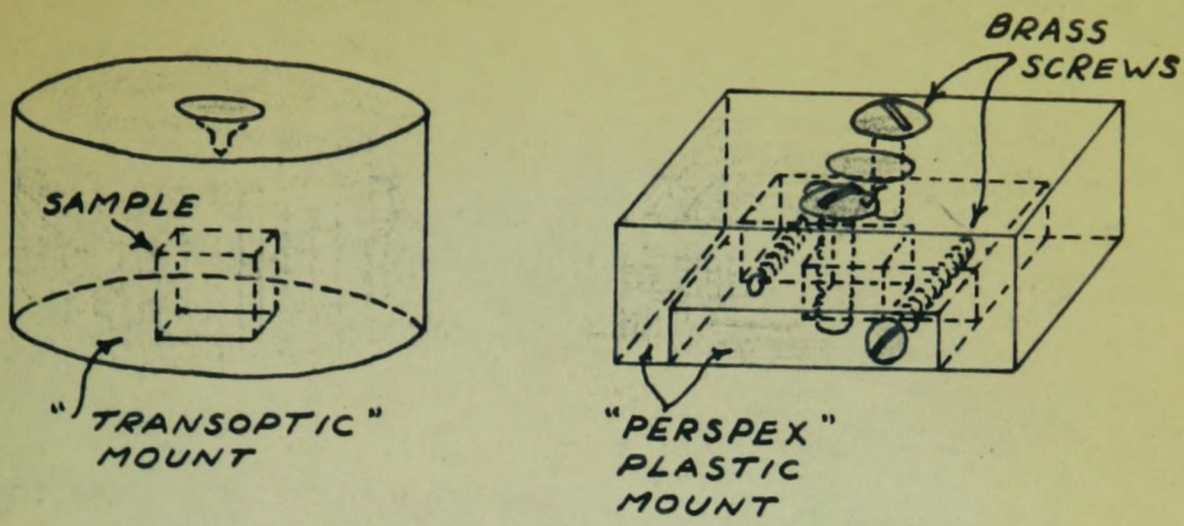

Figure 16: Schematic representation of sample mounts prepared for slurry polishing. X 1½

Figure 17: Photograph of sample holder and polishing wheel used for slurry polishing.

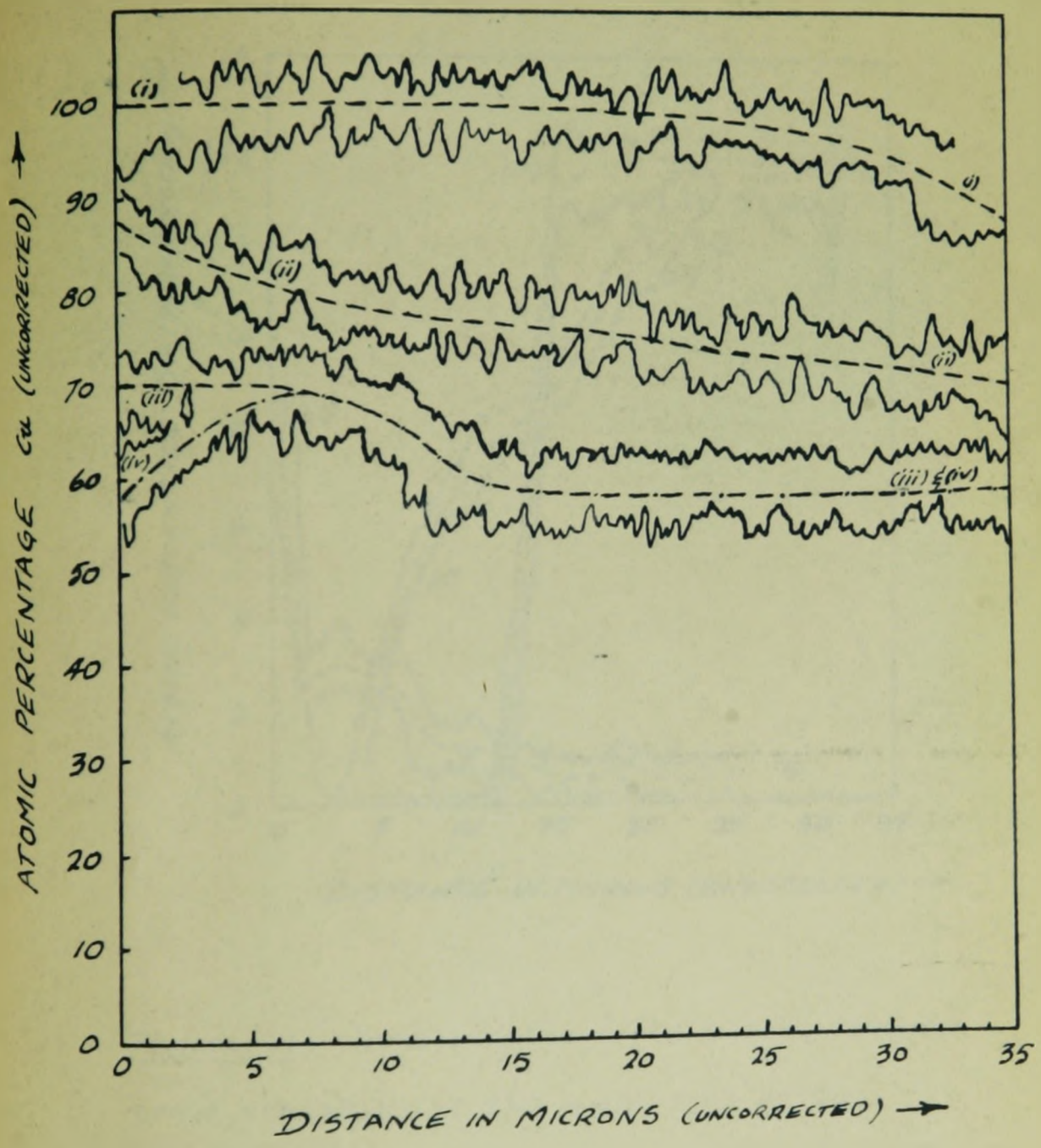

Figure 18: Oscilloscope trace during electron probe analysis for copper - enlarged during reproduction.

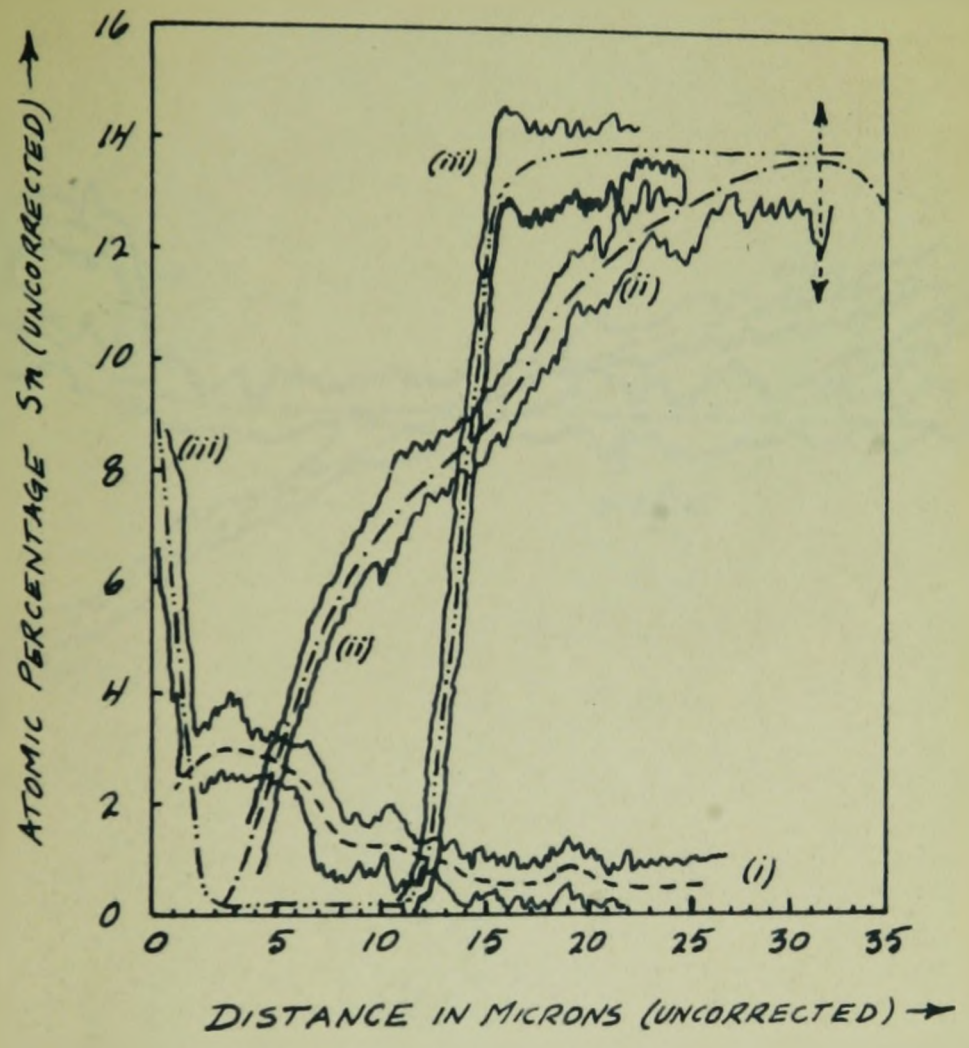

Figure 19: Oscilloscope trace during electron probe analysis for tin - enlarged during reproduction.

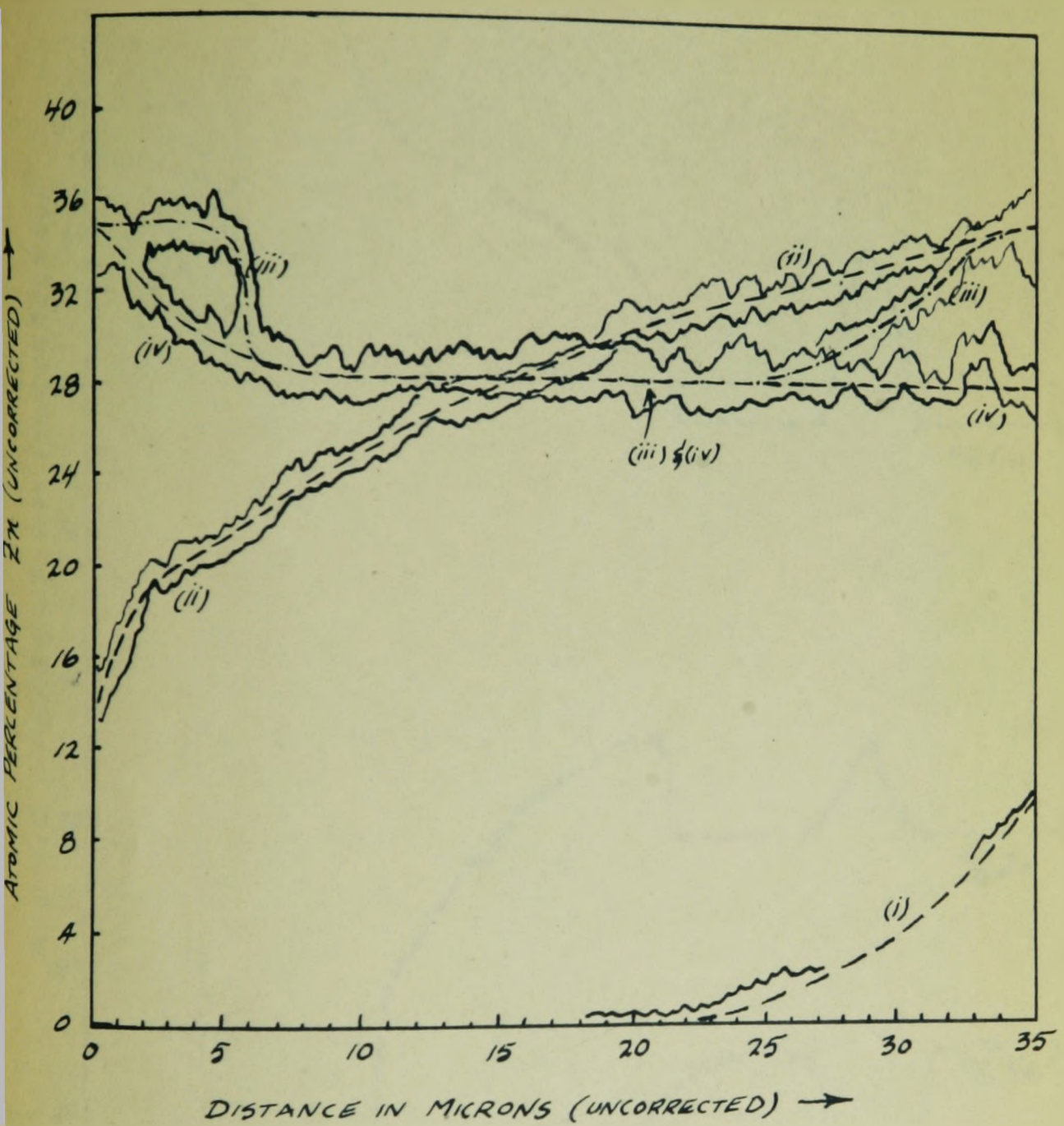

Figure 20: Oscilloscope trace during electron probe analysis for zinc - enlarged during reproduction.

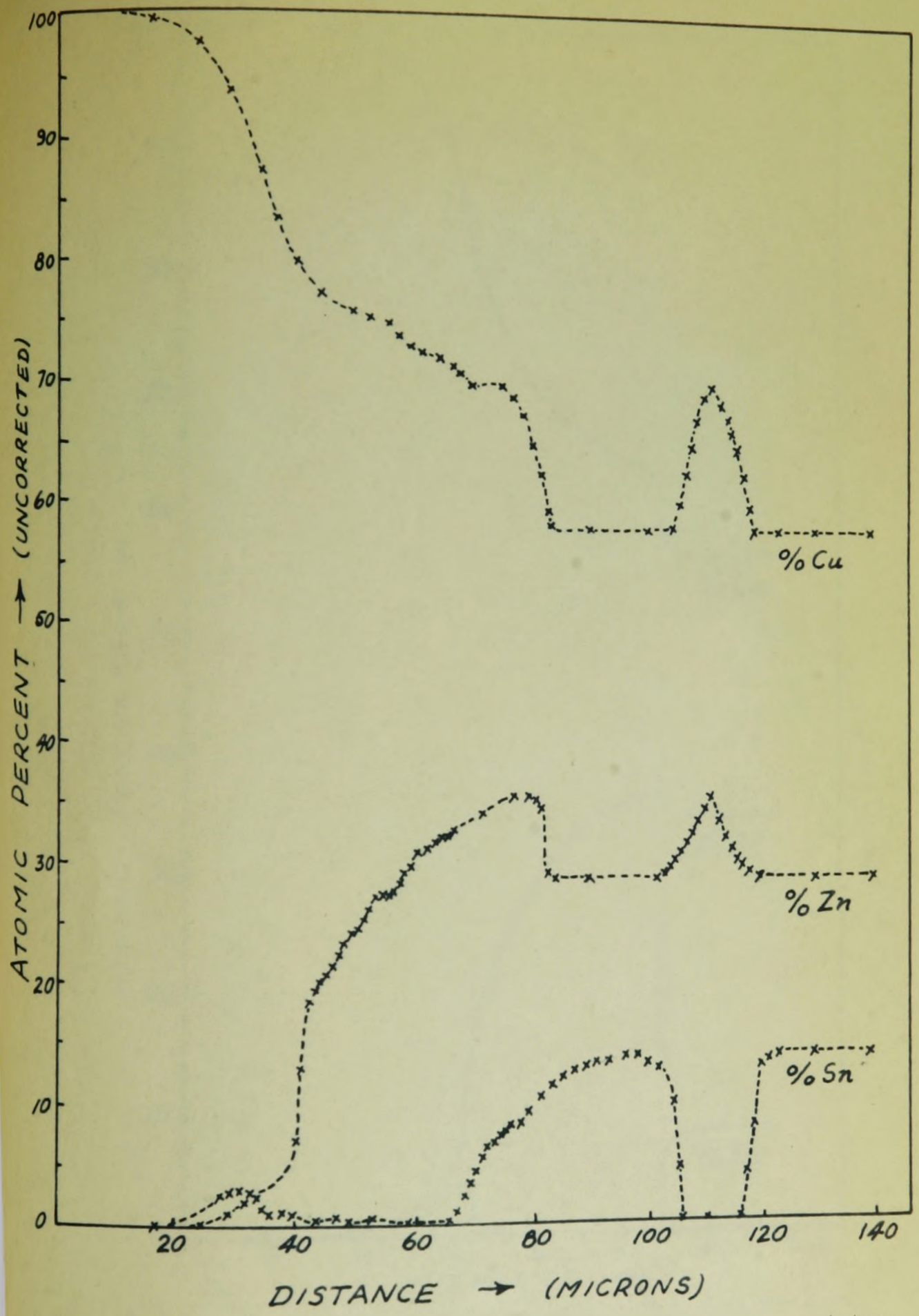

Figure 21: Composition variations with distance as determined from Figures 18, 19 and 20.

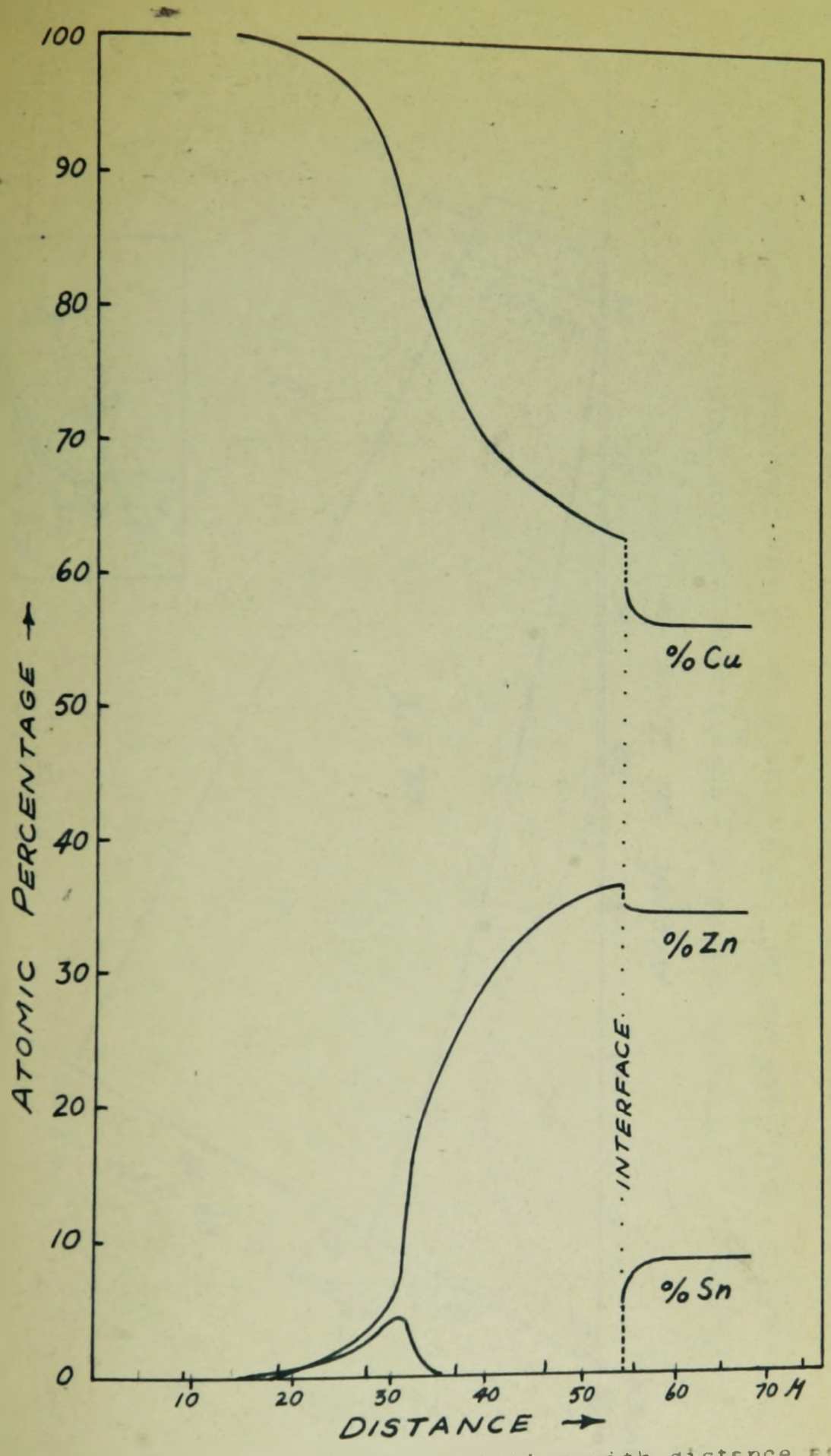

Figure 22: Composition variation with distance as estimated from phase diagram, terminal composition and electron probe microanalyser data.

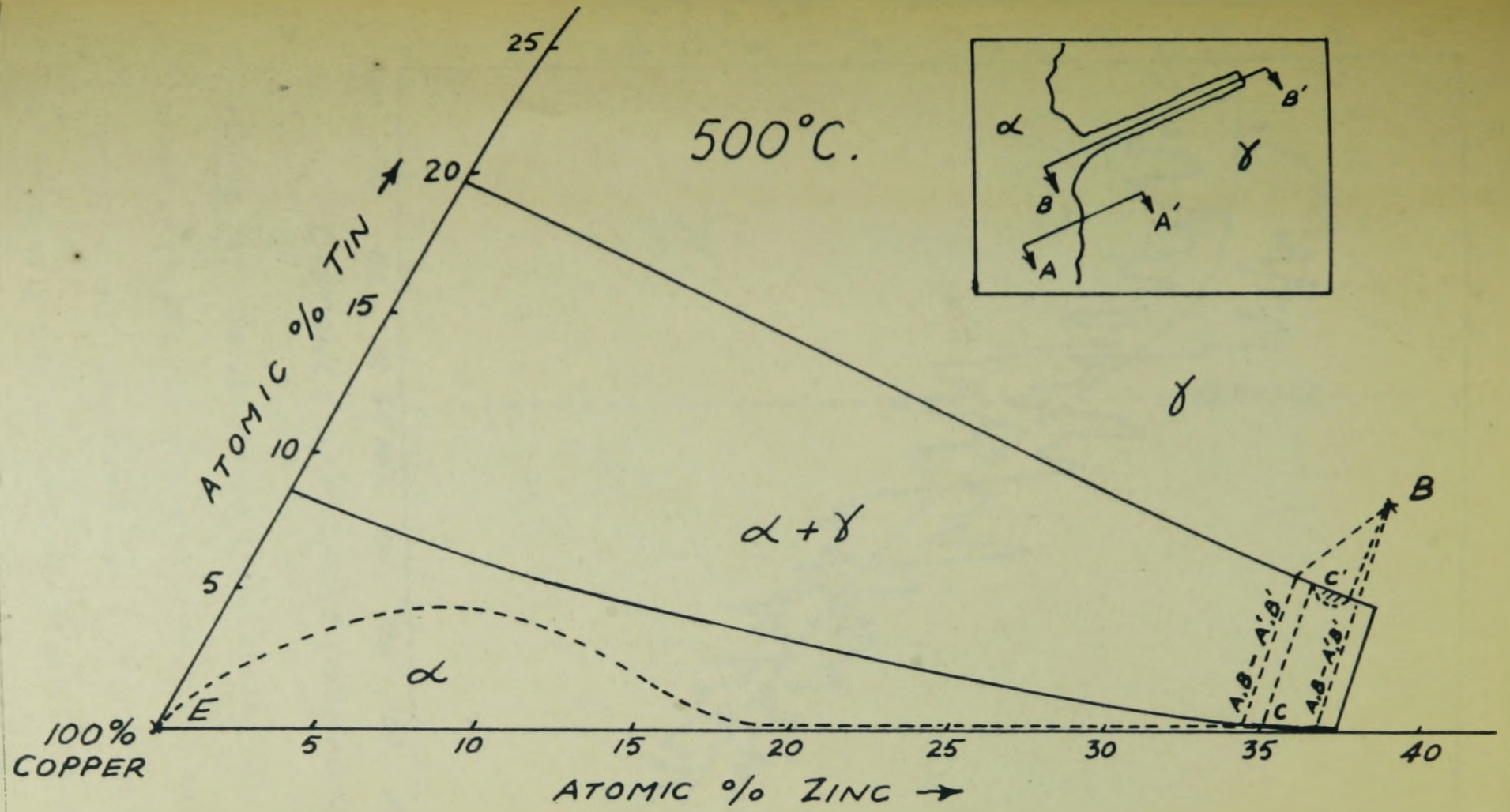

Figure 23: Estimated diffusion - composition path for 100%Cu:Cu-15%Sn-35%Zn couple. Paths AA' and BB' are in the range shown. Path CC' is thought to be representative of an intermediate hypothetical path for a flat interface and shows the presence of a zone of supersaturation.

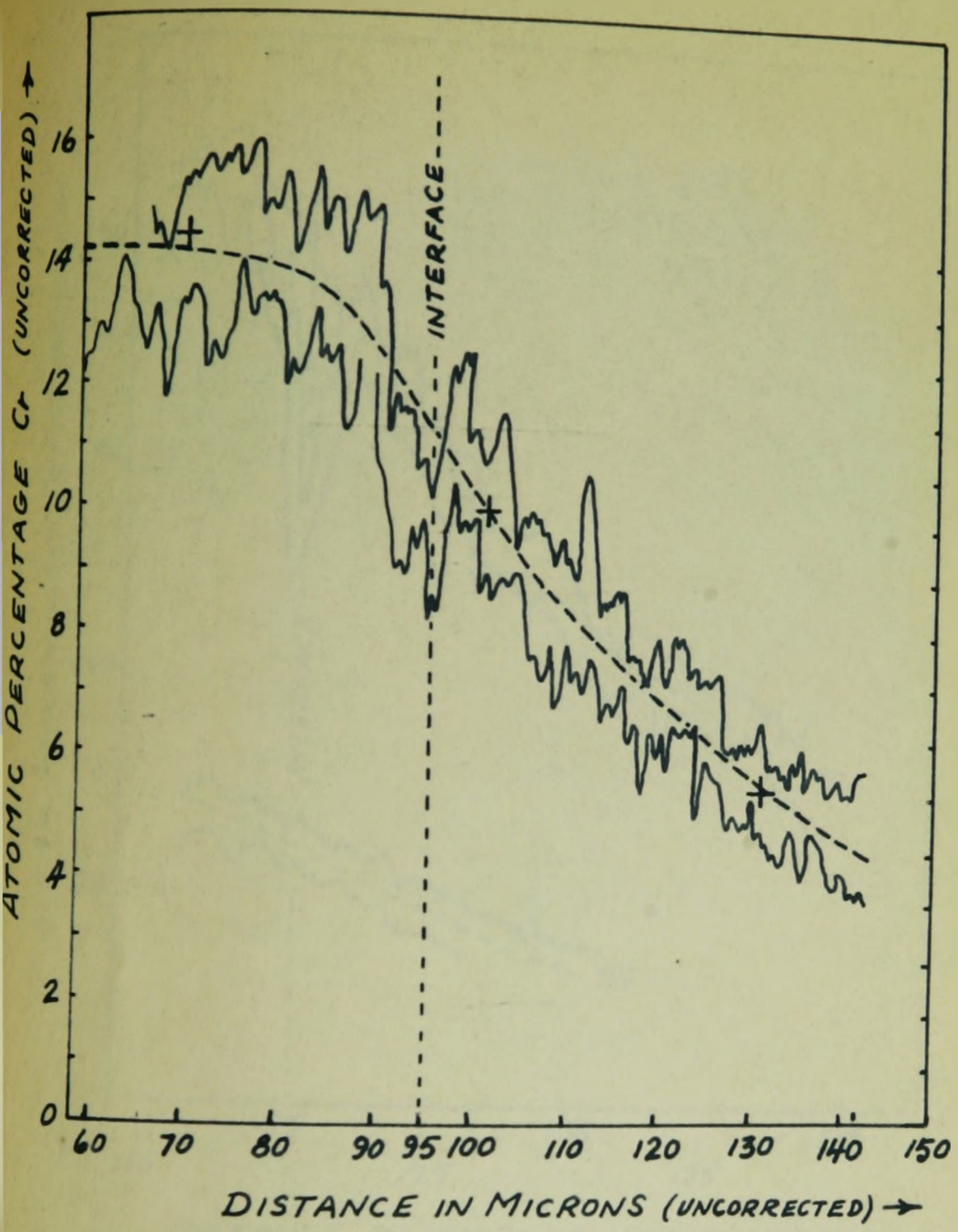

Figure 24: Oscilloscope trace during electron probe analysis for chromium - enlarged during reproduction. The deviation at the interface is evidently due to surface relief. The point-to-point check points are indicated as +.

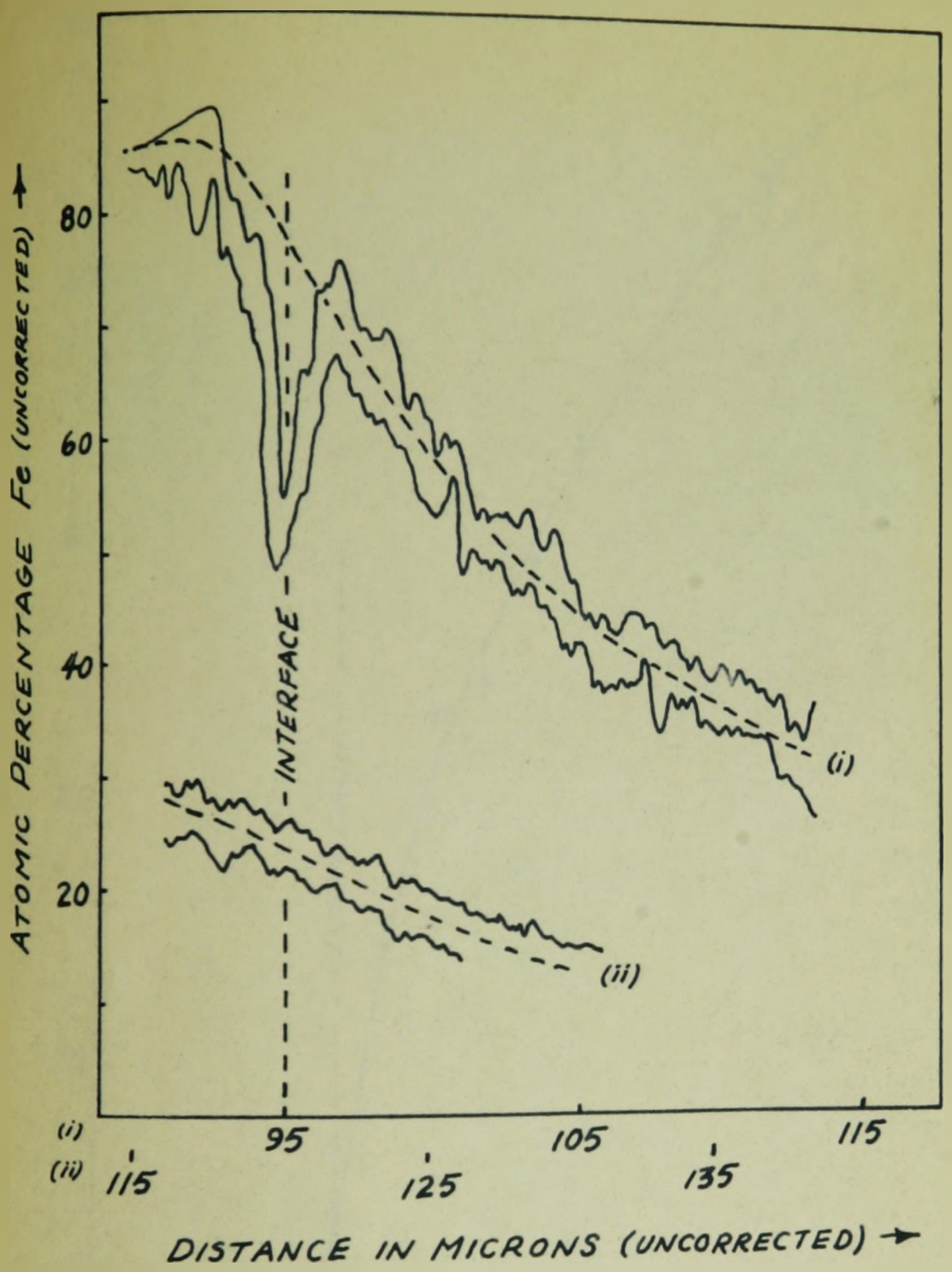

Figure 25: Oscilloscope trace during electron probe analysis for iron - enlarged during reproduction. The deviation evident at the interface is evidently due to surface relief.

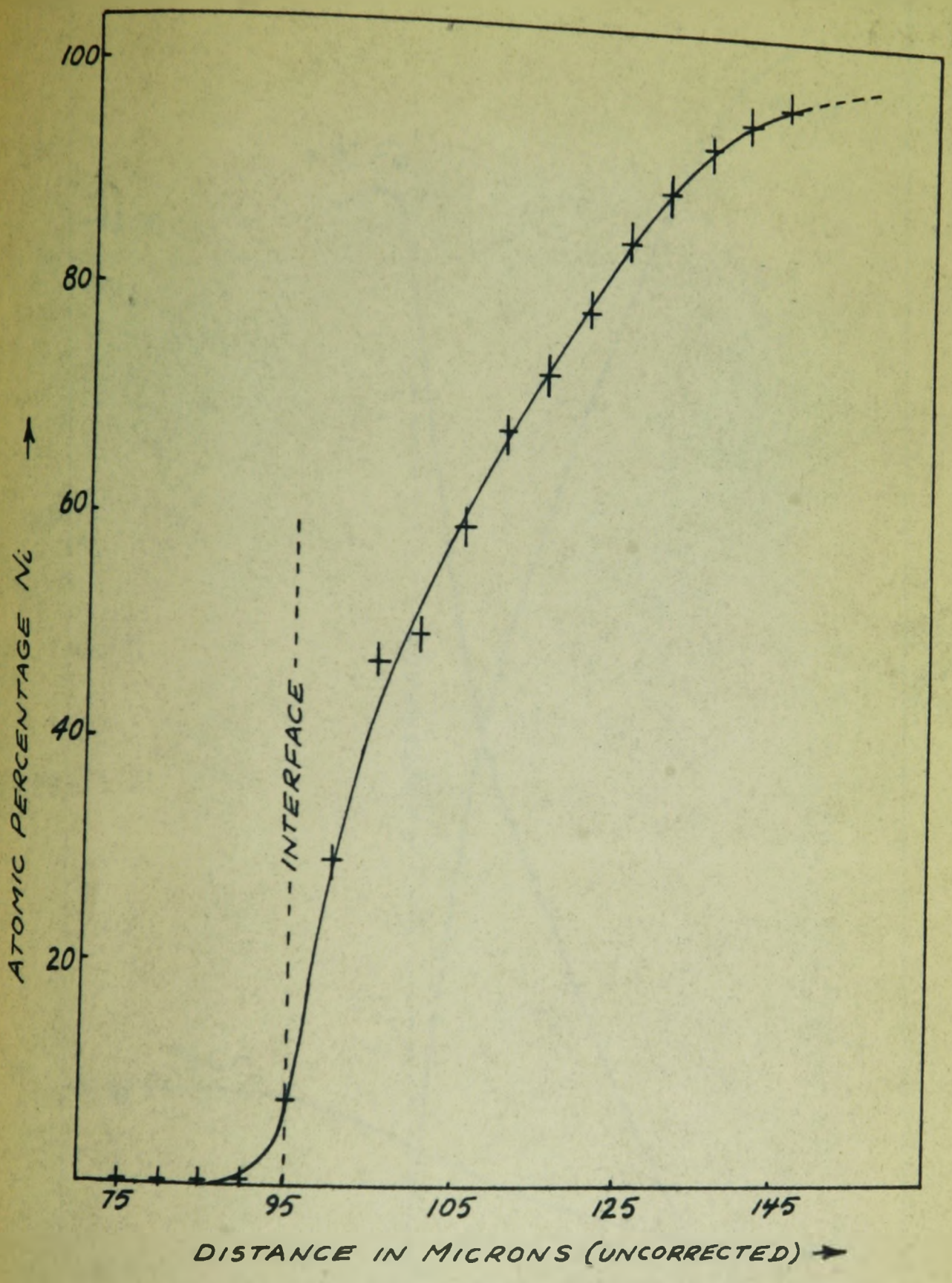

Figure 26: Point-to-point electron probe analysis for nickel plotted as a function of distance.

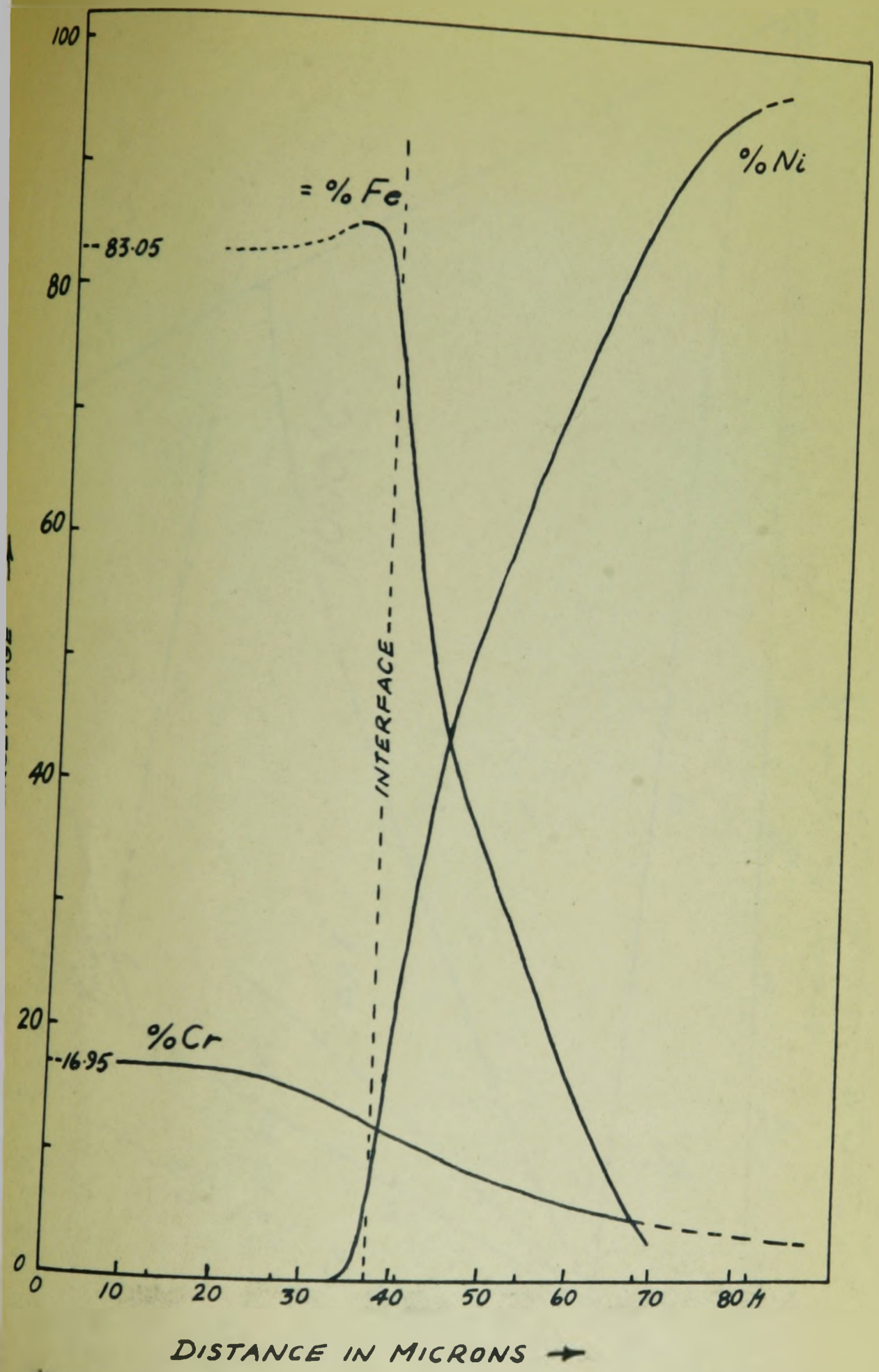

Figure 27: Corrected composition variations with distance as determined from Figures 24 to 26 and analysis.

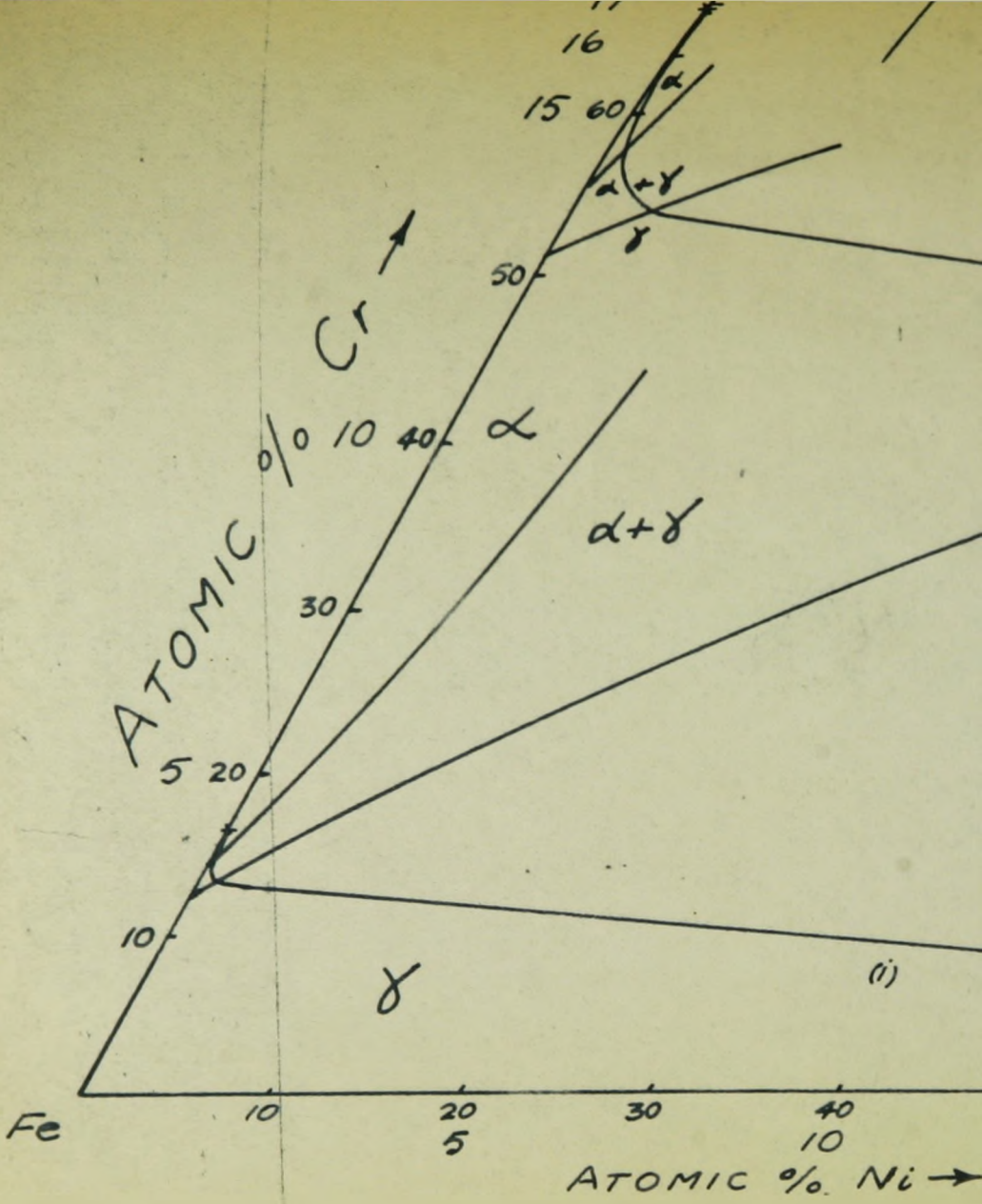

Figure 28: Estimated diffusion

couple. Curve (ii) amplifies th

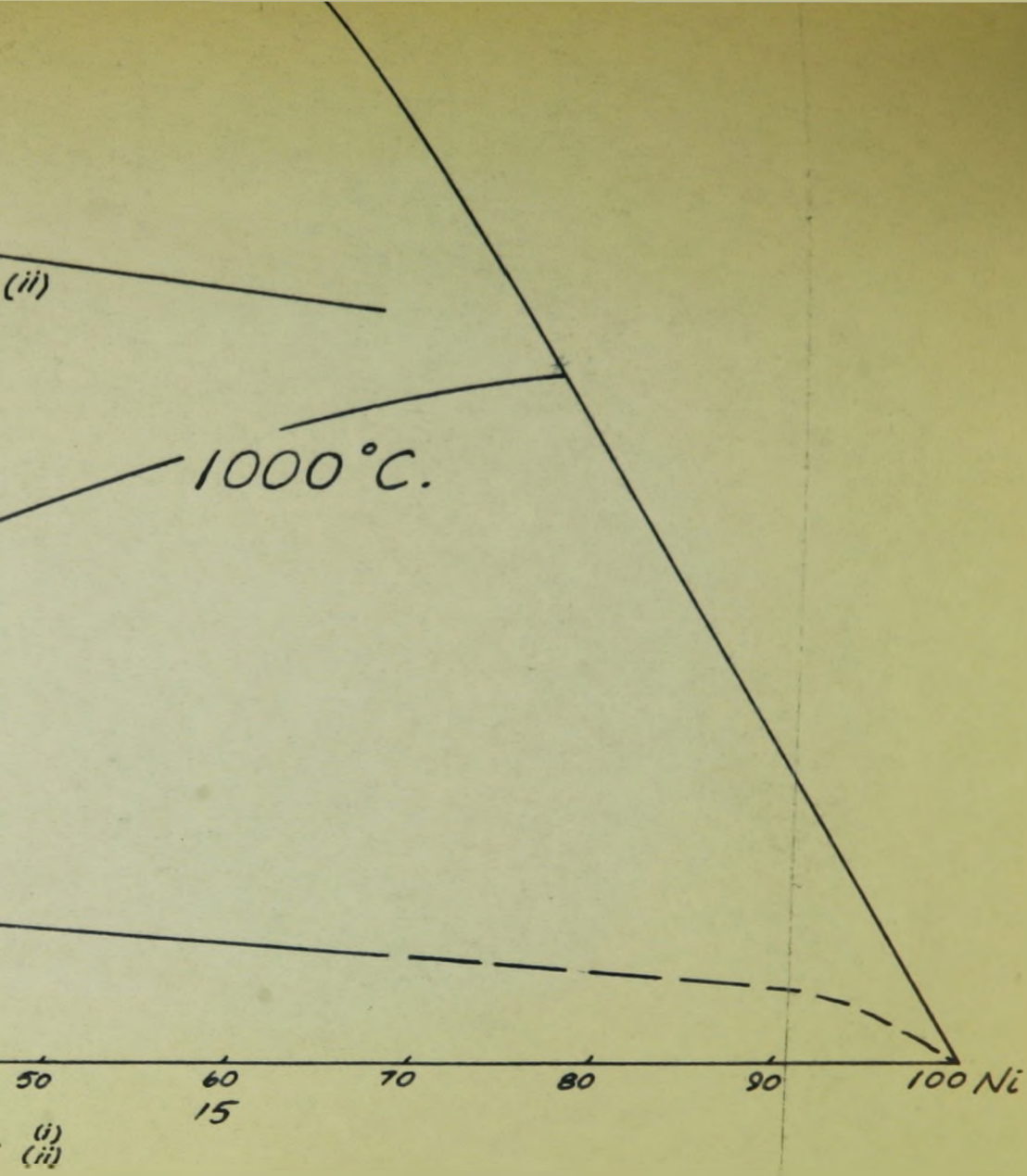

- composition path for Fe-13%Cr:100%Ni

e Fe-13%Cr part of curve (i).

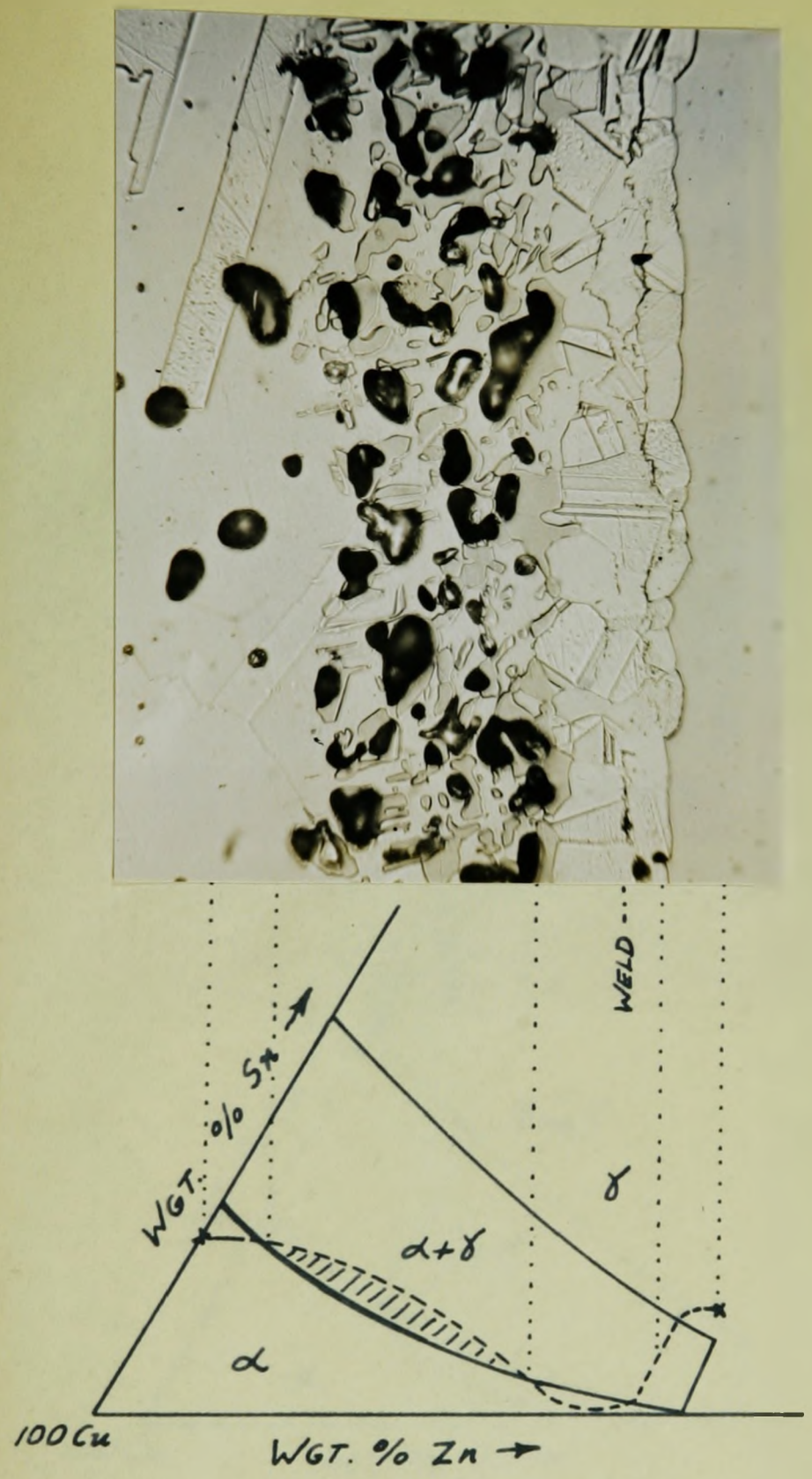

Figure 29: Micrograph of Cu-15%Sn:Cu-15%Sn-35%Zn diffusion couple. 120 hrs. @ 500°C, X560. The estimated composition-diffusion path is included.

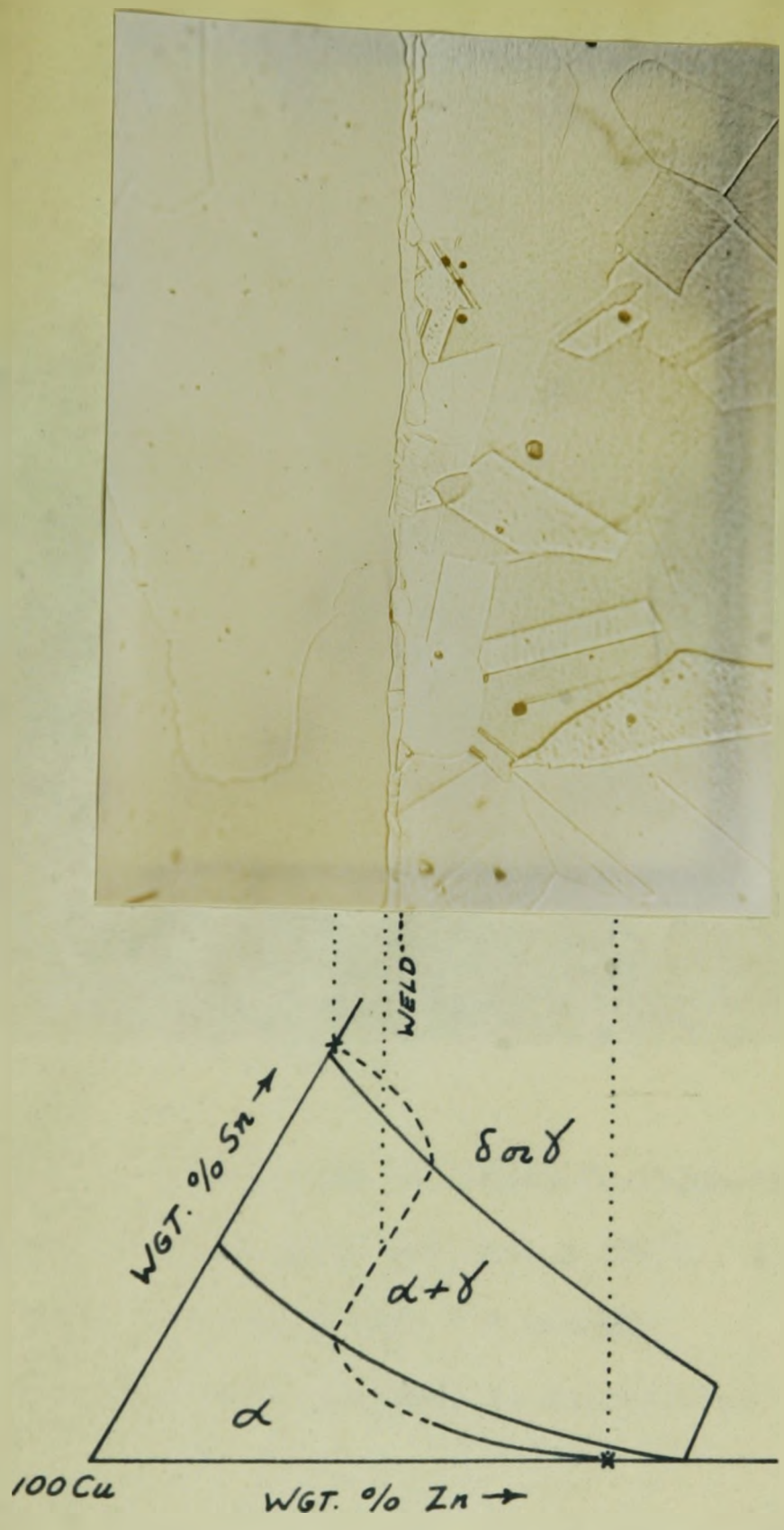

Figure 30: Micrograph of Cu-35%Zn:Cu-32.5%Sn diffusion couple after 24 hrs. @ 500°C, X370. The estimated composition-diffusion path is included.

Figure 31: Micrograph of 100%Cu:Cu-15%Sn-35%Zn diffusion couple after 120 hrs. @ 500°C., X 710. Potassium dichromate etch - 2 seconds.

The electron-probe traverse is illustrated.

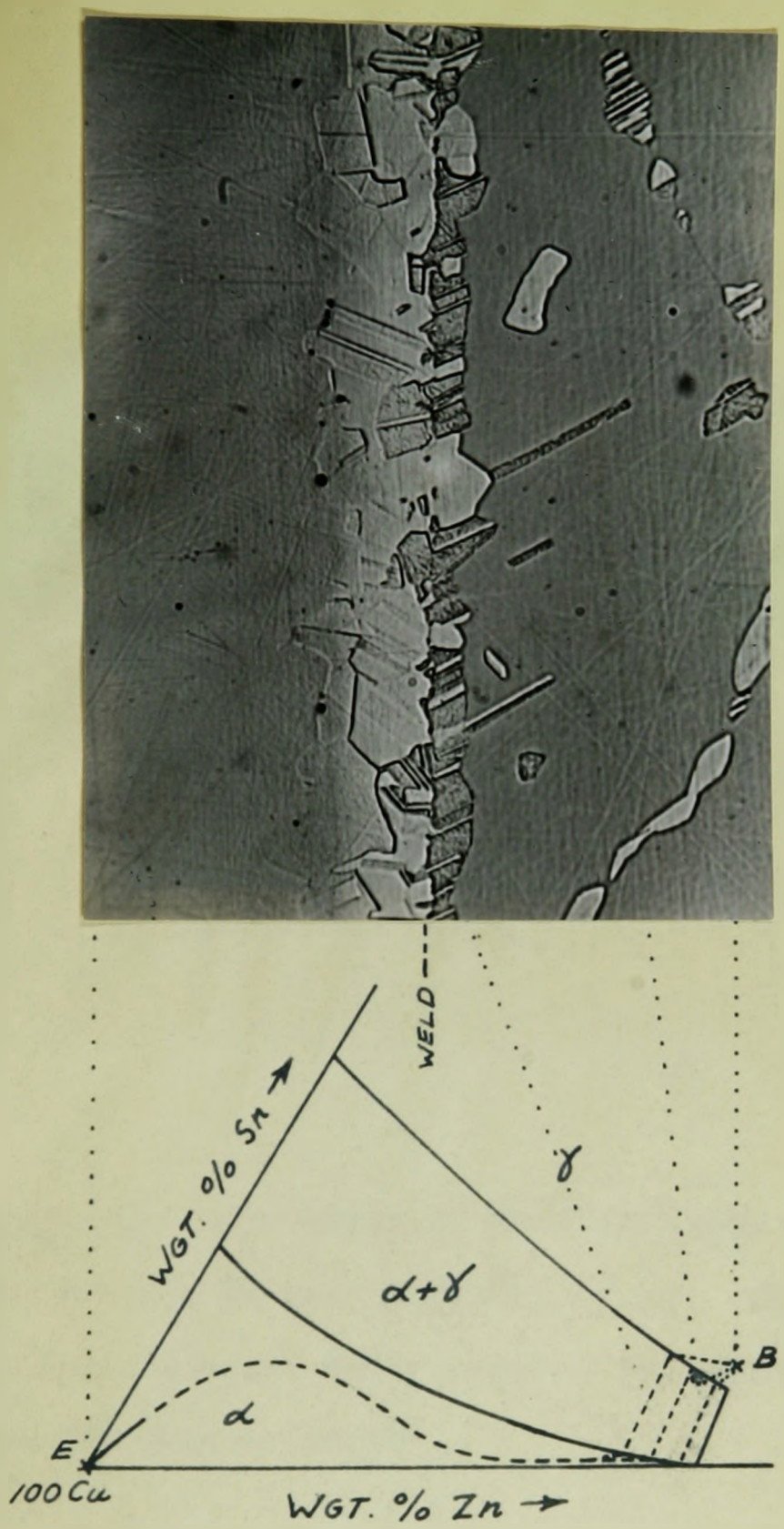

Figure 32: Micrograph of 100%Cu:Cu-15%Sn-35%Zn diffusion couple after 120 hrs. @ 500°C, X370. The estimated composition-diffusion path (Figure 23) is duplicated here.

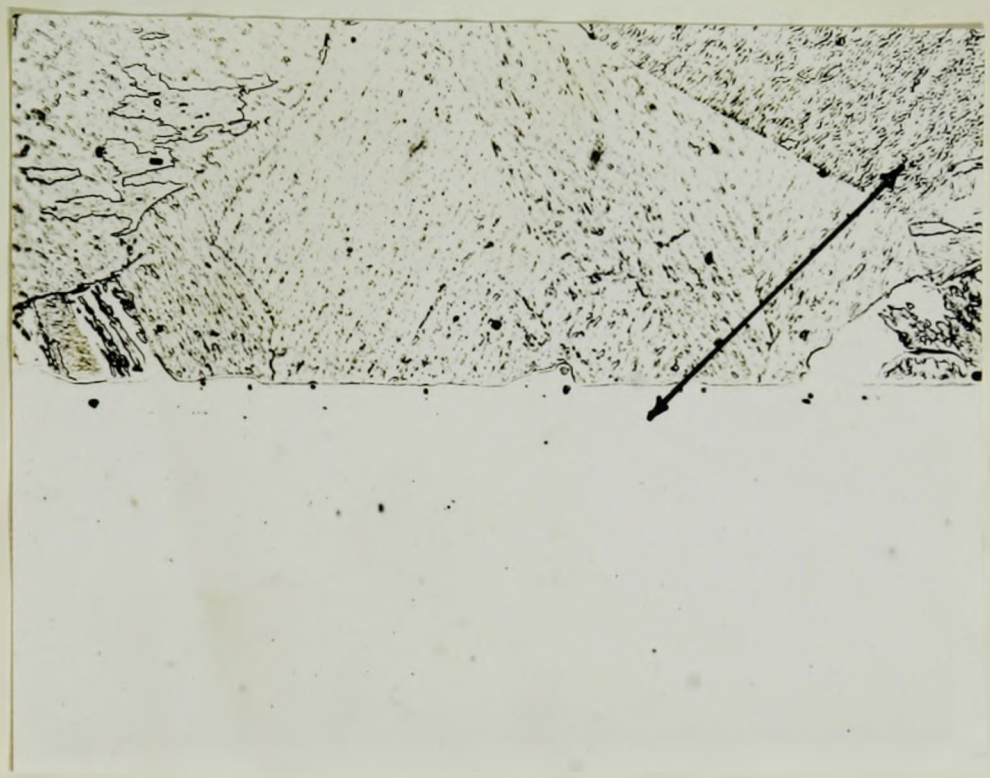

Figure 33: Micrograph of Fe-13%Cr:100%Ni diffusion couple after 24 hrs. @ 1000°C., X 190. Etched in Kalling's reagent for 1 second. The electon-probe scanning path is shown.

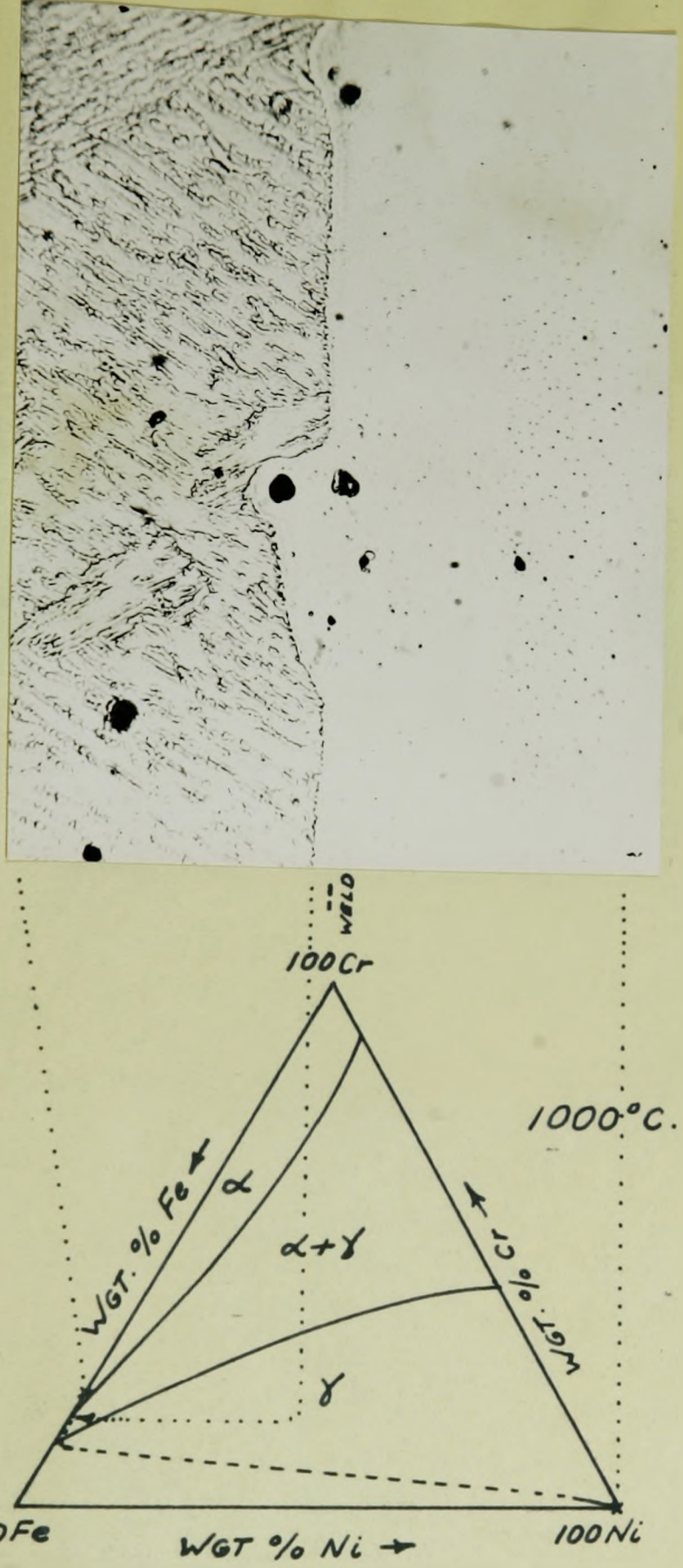

Figure 34: Micrograph of Fe-13%Cr:100%Ni diffusion couple after 24 hrs. @ 1000°C, X755. The estimated composition-diffusion path (Figure 27) is duplicated here.